JPET Fast Forward. Published on June 25, 2012 as DOI: 10.1124/jpet.111.191239

Effect of Fasudil, a selective inhibitor of Rho Kinase activity, in the secondary injury associated with the experimental model of spinal cord trauma

Daniela Impellizzeri, Emanuela Mazzon, Irene Paterniti, Emanuela Esposito, Salvatore Cuzzocrea

Department of Clinical and Experimental Medicine and Pharmacology, School of Medicine, University of Messina, Italy

E. M.; E. S.; S.C. IRCCS Centro Neurolesi "Bonino-Pulejo", Messina, Italy

D.I.;E.S.;I.P; S.C. Department of Clinical and Experimental Medicine and Pharmacology, School of Medicine, University of Messina, Italy

JPET Fast Forward. Published on June 25, 2012 as DOI: 10.1124/jpet.111.191239
This article has not been copyedited and formatted. The final version may differ from this version.

Author for correspondence: Prof. Salvatore Cuzzocrea, Department of Clinical and Experimental Medicine and Pharmacology, School of Medicine, University of Messina, Torre Biologica – Policlinico Universitario Via C. Valeria – Gazzi – 98100 Messina Italy; Tel.: 090 2213644, Fax.: 090 2213300; email: salvator@unime.it.

Number of text pages: 41

Number of figures: 10

Number of references: 56

Number of words in the Abstract: 222

Number of words in the Introduction: 698

Number of words in the Discussion: 1552

Nonstandard abbreviations: Spinal Cord Injury (SCI); nitric oxide (NO); reactive oxygen species (ROS); nuclear factor-κB (NF-κB); mitogen-activated protein kinase (MAPK); rho-kinase (ROK); 1-(5-isoquinolinesulfonyl)-homopiperazine hydrochloride, (Fasudil, or HA-1077); tumor Necrosis Factor (TNF-α); interleukin-1β (IL-1β); poly-ADP-ribose (PAR); poly-ADP-ribose polymerase (PARP); glial fibrillary acidic protein (GFAP); myeloperoxidase activity (MPO); peroxynitrite ($ONOO^-$), NOD-like receptor family, pyrin domain-containing 3, (NLRP3), myosin-binding subunit, myosin phosphate target subunit-1 (MYPT1).

Running title: Fasudil and spinal cord injury

Section: Neuropharmacology

JPET Fast Forward. Published on June 25, 2012 as DOI: 10.1124/jpet.111.191239
This article has not been copyedited and formatted. The final version may differ from this version.

Abstract

Rho kinase (ROK) may play an important role in regulating biological events of cells, including proliferation, differentiation and survival/death. Blockade of ROK promotes axonal regeneration and neuron survival in vivo and in vitro, thereby exhibiting potential clinical applications in spinal cord damage and stroke. The aim of this experimental study was to determine the role of ROK signaling pathways in the inflammatory response, in particular in the secondary injury associated with the experimental model of spinal cord trauma. The injury was induced by application of vascular clips to the dura via a four-level T5-T8 laminectomy in mice. Fasudil was administered in mice (10 mg/kg i.p.) 1 h and 6 h after the trauma. The treatment with fasudil significantly decreased (1) histological damage, (2) motor recovery, 3) nuclear factor (NF)-κB expression, (4) rho kinase (ROK) activity, (5) inflammasome activation (caspase 1 and NOD-like receptor family, pyrin domain-containing 3, NLRP3 expression), (6) pro-inflammatory cytokines production such as tumor necrosis factor (TNF-α) and interleuchin-1β (IL-1β), (7) neutrophil infiltration, (8) nitrotyrosine and poly-ADP-ribose (PAR) formation, (9) glial fibrillary acidic protein (GFAP) expression, (10) apoptosis (TUNEL staining, FAS ligand expression, Bax and Bcl-2 expression), (11) MAP kinase activation (P-ERK and P-JNK expression). Our results indicate that inhibition of ROK by fasudil may represent a useful therapeutic perspective in the treatment of inflammation associated with spinal cord trauma.

JPET Fast Forward. Published on June 25, 2012 as DOI: 10.1124/jpet.111.191239
This article has not been copyedited and formatted. The final version may differ from this version.

Introduction

Individuals paralyzed by Spinal Cord Injury (SCI) are left with one of the most physically disabling and psychologically devastating conditions known to humans. Over 10.000 North Americans, most of them under the age of 30 years, experience such an injury each year (Nobunaga et al., 1999). Although enormous economic impact for the medical, surgical and rehabilitative care, the complex pathophysiology of SCI leads to the difficulty in finding a suitable therapy (Stover and Fine, 1987). Typically, the centre of the spinal cord injury is predominantly characterized by necrotic death. The primary injury refers to the mechanical damage leading to direct cell death and bleeding. Further progressive destruction of the tissue surrounding the necrotic core is known as secondary injury (Beattie et al., 2000) that is determined by a large number of vascular, biochemical and cellular cascades including the breakdown of blood-spinal cord barrier with edema formation, ischaemia and hypoxia, the release of vasoactive substances leading to alteration of spinal cord perfusion, the excitotoxicity leading to Ca^{2+} dependent, glutamate-associated neuronal cell death, the formation of free radicals and nitric oxide (NO), a damage of mitochondrias with energy depletation, the invasion and activation of inflammatory cells such as (neutrophils, resident microglia, peripheral macrophages and astrocytes) which secrete lytic enzymes and cytokines contributing to further tissue damage, the apoptosis of oligodendrocytes and neurodegeneration (Hausmann, 2003).

Neutrophils are the first inflammatory cells to arrive at the site of injury in non neuronal and neuronal tissue. Neutrophils are involved in the modulation of the secondary injury by release of neutrophil proteases and reactive oxygen species (ROS) (Hausmann, 2003), which activate the transcription factors such as nuclear factor-κB (NF-κB) that plays a central and crucial role in inducing the expression of inflammatory cytokines (Chen et al., 2004). Increased ROS production is also implicated in the development of cellular hypertrophy and remodeling, at

least in part through activation of redox-sensitive protein kinases such as the mitogen-activated protein kinase (MAPK) superfamily (Li et al., 2002). In addition, the generation of ROS seems also critical for the activation of the NLRP3 inflammasome (Dostert et al., 2009).

Ras-homologus (Rho) signaling pathways, which likely serve homeostatic functions under normal physiological conditions, appear to be most highly activated under conditions of inflammation and injury. Whereas their recruitment may be of benefit for initiation of protective responses, their sustained activation may have pathological consequences (Seasholtz and Brown, 2004).

Small (21 kDa) guanosine triphosphatases (GTPases) of the Rho family and one of their effectors, Rho-kinase (ROK) are known to act as molecular switches controlling several critical cellular functions, such as actin cytoskeleton organization, cell adhesion, migration, ROS formation and apoptosis, as well as cytokinesis and oncogenic transformation (Riento and Ridley, 2003; Bokoch, 2005). There are two isoforms of ROK, known as ROK I and II. ROK I shows the highest expression level in non neuronal tissues, whereas ROK II is preferentially expressed in the brain (Wang et al., 2011). Moreover, ROK inhibitors have been shown to be effective against reperfusion injury in the liver (Shiotani et al., 2004), heart (Bao et al., 2004), tissue fibrosis (Bourgier et al., 2005), cerebral ischemia (Satoh et al., 2001) and pulmonary hypertension (Abe et al., 2004).

Fasudil, or 1-(5-isoquinolinesulfonyl)-homopiperazine hydrochloride, (HA-1077) is a specific ROK inhibitor (He et al., 2008) and is the first kinase inhibitor drug used in a clinical setting in Japan (Shibuya et al., 1992). Fasudil has been used for years for the treatment of subarachnoid hemorrhage, and its safety for clinical use is well established. Fasudil has been reported to inhibit NF-κB signaling following infection with the human immunodeficiency virus (Sato et al., 1998). NF-κB is normally sequestered in the cytoplasm, bound to regulatory proteins IκBs. In response to a wide range of stimuli including oxidative stress, infection,

hypoxia, extracellular signals, and inflammation, IκB is phosphorylated by the enzyme IκB kinase (Bowie and O'Neill, 2000). The net result is the release of the NF-κB dimer, which is then free to translocate into the nucleus and to active genic transcription of inflammatory proteins.

The aim of the present study was to determine the role of ROK signaling pathways in the inflammatory response, in particular in the secondary injury associated with spinal cord trauma.

JPET Fast Forward. Published on June 25, 2012 as DOI: 10.1124/jpet.111.191239
This article has not been copyedited and formatted. The final version may differ from this version.

Methods

Animals

Male Adult CD1 mice (25-30g, Harlan Nossan, Milan, Italy) were housed in a controlled environment and provided with standard rodent chow and water. Animal care was in compliance with Italian regulations on protection of animals used for experimental and other scientific purpose (D.M. 116192) as well as with the EEC regulations (O.J. of E.C. L 358/1 12/18/1986).

SCI

Mice were anaesthetized using chloral hydrate (400 mg/kg body weight). We used the clip compression model described by Rivlin and Tator (Rivlin and Tator, 1978). A longitudinal incision was made on the midline of the back, exposing the paravertebral muscles. These muscles were dissected away exposing T5-T8 vertebrae. The spinal cord was exposed via a four-level T5-T8 laminectomy and SCI was produced by extradural compression of the spinal cord using an aneurysm clip with a closing force of 24 g. In the injured groups, the cord was compressed for 1 min. Following surgery, 1.0 cc of saline was administered subcutaneously in order to replace the blood volume lost during the surgery. During recovery from anesthesia, the mice were placed on a warm heating pad and covered with a warm towel. The mice were singly housed in a temperature-controlled room at 27°C for a survival period of 10 days. Food and water were provided to the mice ad libitum. During this time period, the animals' bladders were manually voided twice a day until the mice were able to regain normal bladder function. Sham injured animals were only subjected to laminectomy.

Experimental Design

Mice were randomized into 4 groups of 20 mice/group (N=80 total animals). 40 mice were sacrificed at 24 h after SCI in order to evaluate the various parameter, while other 40 were observed until 10 days after SCI in order to evaluate the motor score. Sham animals were subjected to the surgical procedure except that the aneurysm clip was not applied and treated intraperitoneally (i.p.) with vehicle (saline) or Fasudil (10 mg/kg) 1 and 6 h after surgical procedure. The remaining mice were subjected to SCI (as described above) and treated with an i.p. bolus of vehicle (saline) or Fasudil 1 h and 6 h after SCI.

The dose was chosen on based of recent studies (Ding et al.,2011 ; Ma et al., 2011).

Light microscopy

Spinal cord tissues were taken at 24 h following trauma. Tissue segments containing the lesion (1 cm on each side of the lesion) were paraffin embedded and cut into 5 μm-thick sections. Tissue sections (thickness 5 μm) were deparaffinised with xylene, stained with Haematoxylin/Eosin (H&E), or with silver impregnation for reticulum and studied using light microscopy (Dialux 22 Leitz). The segments of each spinal cord were evaluated by an experienced histopathologist. Damaged neurons were counted and the histopathology changes of the gray matter were scored on a 6-point scale (Sirin et al., 2002): 0, no lesion observed, 1, gray matter contained 1 to 5 eosinophilic neurons; 2, gray matter contained 5 to 10 eosinophilic neurons; 3, gray matter contained more than 10 eosinophilic neurons; 4, small infarction (less than one third of the gray matter area); 5, moderate infarction; (one third to one half of the gray matter area); 6, large infarction (more than half of the gray matter area). The scores from all the sections from each spinal cord were averaged to give

a final score for individual mice. All the histological studies were performed in a blinded fashion.

Measurement of spinal cord TNF-α and IL-1β levels

Portions of spinal cord tissues, collected at 24 hours after SCI, were homogenized as previously described in phosphate buffered saline (PBS) containing 2 mmol/L of phenyl-methyl sulfonyl fluoride (PMSF, Sigma Chemical Co.) and tissue TNF-α and IL-1β levels were evaluated. The assay was carried out by using a colorimetric, commercial kit (Calbiochem-Novabiochem Corporation, USA) according to the manufacturer instructions. All TNF-α and IL-1β determinations were performed in duplicate serial dilutions.

Myeloperoxidase activity

Myeloperoxidase (MPO) activity, an indicator of polymorphonuclear leukocyte (PMN) accumulation, was determined in the spinal cord tissues as previously described (Mullane, 1989) at 24 hours after SCI. Following SCI, spinal cord tissues were obtained and weighed and each piece homogenized in a solution containing 0.5 % (w/v) hexadecyltrimethyl-ammonium bromide dissolved in 10 mM potassium phosphate buffer (pH 7) and centrifuged for 30 min at 20,000 x g at 4°C. An aliquot of the supernatant was then allowed to react with a solution of 1.6 mM tetramethylbenzidine and 0.1 mM H_2O_2. The rate of change in absorbance was measured spectrophotometrically at 650 nm. MPO activity was defined as the quantity of enzyme degrading 1 µmol of peroxide per min at 37°C and was expressed as units of MPO/mg of proteins.

JPET Fast Forward. Published on June 25, 2012 as DOI: 10.1124/jpet.111.191239
This article has not been copyedited and formatted. The final version may differ from this version.

Grading of motor disturbance

The motor function of mice subjected to compression trauma was assessed once a day for 10 days after injury. Recovery from motor disturbance was graded using the Basso Mouse Scale (BMS) (Basso et al., 2006).

Immunohistochemical localization of TNF-α, IL-1β, nitrotyrosine, PAR, FAS ligand, Bax, Bcl-2, GFAP and P-JNK

At 24 h after SCI, the tissues were fixed in 10% (w/v) PBS-buffered formaldehyde and 8 mm sections were prepared from paraffin embedded tissues. After deparaffinization, endogenous peroxidase was quenched with 0.3% (v/v) hydrogen peroxide in 60% (v/v) methanol for 30 min. The sections were permeabilized with 0.1% (w/v) Triton X-100 in PBS for 20 min. Non-specific adsorption was minimized by incubating the section in 2% (v/v) normal goat serum in PBS for 20 min. Endogenous biotin or avidin binding sites were blocked by sequential incubation for 15 min with avidin-biotin peroxidase complex (DBA). Sections were incubated overnight with 1) goat polyclonal anti-TNF-α antibody (1:100 in PBS, wt/vol) (Santa Cruz Biotechnology.INC), 2) rabbit polyclonal anti-IL-1β (1:100 in PBS, wt/vol) (Santa Cruz Biotechnology.INC), 3) rabbit polyclonal anti-Bax (1:100 in PBS, wt/vol) (Santa Cruz Biotechnology.INC), 4) rabbit polyclonal anti-Bcl-2 (1:100 in PBS, wt/vol) (Santa Cruz Biotechnology.INC), 5) goat polyclonal anti-PAR antibody (1:100 in PBS, wt/vol) (Santa Cruz Biotechnology.INC), 6) mouse monoclonal anti Fas Ligand (1:100 in PBS, wt/vol) (Monosan), mouse monoclonal anti-GFAP (1:100 in PBS, wt/vol) (Santa Cruz Biotechnology.INC), 9) rabbit polyclonal anti- nitrotyrosine (1:250 in PBS, wt/vol) (Millipore), mouse monoclonal anti P-JNK (1:100 in PBS, wt/vol) (Santa Cruz Biotechnology.INC). Sections were washed with PBS, and incubated with secondary

antibody. Specific labeling was detected with a biotin-conjugated goat anti-rabbit IgG and DBA. The counter stain was developed with DAB (brown colour) and nuclear fast red (red background). A positive staining (brown colour) was found in the sections, indicating that the immunoreactions were positive. To verify the binding specificity for nitrotyrosine, TNF- α, IL-1β, nitrotyrosine, PAR, FAS-L, Bax, and Bcl-2, GFAP and P-JNK, some sections were also incubated with only the primary antibody (no secondary) or with only the secondary antibody (no primary). In these situations no positive staining was found in the sections indicating that the immunoreactions were positive in all the experiments carried out. Immunocytochemistry photographs (N=5) were assessed by densitometry using Imaging Densitometer (AxioVision, Zeiss, Milan, Italy) and a computer program.

Terminal Deoxynucleotidyltransferase-Mediated UTP End Labeling (TUNEL) Assay

TUNEL assay was conducted by using a TUNEL detection kit according to the manufacturer's instruction (Apotag, HRP kit DBA, Milan, Italy). Sections were incubated with 15 µg/ml proteinase K for 15 min at room temperature and then washed with PBS. Endogenous peroxidase was inactivated by 3% H_2O_2 for 5min at room temperature and then washed with PBS. Sections were immersed in terminal deoxynucleotidyltransferase (TdT) buffer containing deoxynucleotidyl transferase and biotinylated dUTP in TdT buffer, incubated in a humid atmosphere at 37°C for 90 min, and then washed with PBS. The sections were incubated at room temperature for 30 min with anti-horseradish peroxidase-conjugated antibody, and the signals were visualized with diaminobenzidine. The number of TUNEL positive cells/high-power field was counted in 5 to 10 fields for each coded slide.

JPET Fast Forward. Published on June 25, 2012 as DOI: 10.1124/jpet.111.191239
This article has not been copyedited and formatted. The final version may differ from this version.

Western blot analysis for IκB-α, NF-κB p65, caspase 1, NLRP3, pi-MYPT1, Bax, Bcl-2, P-ERK and P-JNK kinases

Cytosolic and nuclear extracts were prepared as previously described (Bethea et al., 1998) with slight modifications. Spinal cord tissues from each mouse were suspended in extraction Buffer A containing 0.2 mM PMSF, 0.15 μM pepstatin A, 20 μM leupeptin, 1mM sodium orthovanadate, homogenized at the highest setting for 2 min, and centrifuged at 1,000 x g for 10 min at 4° C. Supernatants represented the cytosolic fraction. The pellets, containing enriched nuclei, were re-suspended in Buffer B containing 1% Triton X-100, 150 mM NaCl, 10 mM TRIS-HCl pH 7.4, 1 mM EGTA, 1 mM EDTA, 0.2 mM PMSF, 20 μm leupeptin, 0.2 mM sodium orthovanadate. After centrifugation 30 min at 15.000 x g at 4° C, the supernatants containing the nuclear protein were stored at -80° C for further analysis. The levels of IκB-α, caspase 1, myosin-binding subunit, myosin phosphate target subunit-1 (pi-MYPT1), NLRP3, Bax, Bcl-2, P-ERK and Phospho-JNK were quantified in cytosolic fraction from spinal cord tissue collected after 24 hours after SCI, while NF-κB p65 levels were quantified in nuclear fraction. The filters were blocked with 1x PBS, 5 % (w/v) non fat dried milk (PM) for 40 min at room temperature and subsequently probed with specific Abs IκB-α (1:1000; Santa Cruz Biotechnology), or anti-Bax (1:500; Santa Cruz Biotechnology), or anti-Bcl-2 (1:500; Santa Cruz Biotechnology), or anti- NF-κB p65 (1:1000; Santa Cruz Biotechnology) or anti–phospho-MYPT1 antibody (1:5000, Upstate, Waltham, MA), anti-NLRP3 (1:200; Santa Cruz Biotechnology, Santa Cruz, CA) or anti- Caspase-1 p10 (1:200, Santa Cruz Biotechnology, CA) or anti P-ERK (1:500; Santa Cruz Biotechnology) or anti-phospho-JNK (1:500; Santa Cruz Biotechnology) in 1x PBS, 5 % w/v non fat dried milk, 0.1 % Tween-20 (PMT) at 4°C, overnight. Membranes were incubated with peroxidase-conjugated bovine anti-mouse IgG secondary antibody or peroxidase-conjugated goat anti-rabbit IgG (1:2000, Jackson ImmunoResearch, West Grove, PA) for 1 h at room temperature. To ascertain that blots were

loaded with equal amounts of proteic lysates, they were also incubated in the presence of the antibody against β-actin (1:10000; Santa Cruz Biotechnology).

The relative expression of the protein bands of IκB-α (~37 kDa), NF-κB p65 (~65 kDa), pi-MYPT1 (~130 kDa), caspase 1 (~46 kDa), NLRP3 (~120 kDa), Bax (~23 kDa), Bcl-2 (~29 kDa), P-ERK (~44 kDa) and phospho-JNK (~46 kDa) was quantified by densitometric scanning of the X-ray films with GS-700 Imaging Densitometer (GS-700, Bio-Rad Laboratories, Milan, Italy) and a computer program (Molecular Analyst, IBM).

Materials

Fasudil was obtained by (LC Laboratories, USA). All compounds were obtained from Sigma-Aldrich Company Ltd. (Milan, Italy). All other chemicals were of the highest commercial grade available. All stock solutions were prepared in non-pyrogenic saline (0.9% NaCl; Baxter, Italy, UK).

Statistical evaluation

All values in the figures and text are expressed as mean ± standard error of the mean (Streit et al.) of N observations. For the in vivo studies, N represents the number of animals studied. In the experiments involving histology or immunohistochemistry, the figures shown are representative at least three experiments (histological or immunohistochemistry coloration) performed on different experimental days on the tissues section collected from all the animals in each group. The results were analyzed by one-way ANOVA followed by a Bonferroni *post-hoc* test for multiple comparisons. A p value of less than 0.05 was considered

significant. BMS scale data were analyzed by the Mann-Whitney test and considered significant when p was <0.05.

Results

Fasudil reduces the severity of spinal cord trauma

The severity of the trauma at the level of the perilesional area, assessed by the presence of edema as well as alteration of the white matter and infiltration of leukocytes, was evaluated 24 h after injury by hematoxylin/eosin (H&E) staining. Significant damage was observed in the spinal cord tissue collected from SCI (Fig. 1 B, B1) when compared with sham-operated mice (Fig. 1 A, A1). Significant protection against the SCI was observed in Fasudil-treated mice (Fig. 1 C, C1). The histological score (Fig. 1 D) was evaluated by an independent observer.

In order to evaluate if histological damage to the spinal cord was associated with a loss of motor function, the modified BMS hind limb locomotor rating scale score was evaluated. While motor function was only slightly impaired in sham mice, mice subjected to SCI had significant deficits in movement (Fig. 1 E). Fasudil treatment significantly ameliorated the functional deficits induced by SCI (Fig. 1 E).

Effect of Fasudil on astrocytic activation

Astrocytes are the major glial cell population within the CNS. After severe activation, astrocytes secrete various neurotoxic substances and express an enhanced level of glial fibrillary acidic protein (GFAP), which is considered a marker protein for astrogliosis (Eng and Ghirnikar, 1994). To investigate the cellular mechanisms by which treatment with Fasudil may attenuate the astrocytic activation during spinal cord injury, we also evaluated the GFAP expression by immunohistochemistry. Spinal cord sections from sham-operated mice did not stain for GFAP (Fig. 2 A, D) whereas spinal cord sections obtained from SCI mice exhibited a

JPET Fast Forward. Published on June 25, 2012 as DOI: 10.1124/jpet.111.191239
This article has not been copyedited and formatted. The final version may differ from this version.

positive staining for GFAP (Fig. 2 B, D). Fasudil treatment reduced the degree of positive staining for GFAP in the spinal cord of mice subjected to SCI (Fig. 2 C, D).

Effect of Fasudil on IκB-α degradation and NF-κB p65 activation.

We evaluated IκB-α degradation, nuclear NF-κB p65 activation by Western Blot analysis to investigate the cellular mechanisms by which treatment with Fasudil may attenuate the development of SCI.

A basal level of IκB-α was detected in the spinal cord from sham-operated animals (Fig. 3 A) whereas IκB-α levels were substantially reduced in SCI mice (Fig. 3 A). Fasudil administration prevented the SCI-induced IκB-α degradation (Fig. 3 A). In addition, NF-κB p65 levels in the nuclear fractions from spinal cord tissue were also significantly increased at 24 h after SCI compared to the sham-operated mice (Fig. 3 B). Fasudil treatment reduced the levels of NF-κB p65 as shown in fig. 3 B.

Effect of Fasudil on caspase 1 and NLRP3 expression.

The NOD-like receptor family, pyrin domain-containing 3 (NLRP3) inflammasome is a caspase-1–containing cytosolic protein complex that is essential for processing and secretion of IL-1β. Thus, to investigate the cellular mechanisms by which treatment with Fasudil may attenuate the inflammasome activation after SCI, we also evaluated caspase 1 and NLRP3 expression by western blot. In spinal cord tissue homogenates after SCI a significant increase in caspase 1 and NLRP3 expression was observed in SCI mice (Fig. 4 A, B). Treatment of mice with Fasudil significantly reduced caspase 1 and NLRP3 expression (Fig. 4 A, B). No expression was observed in sham animals (Fig. 4 A, B).

JPET Fast Forward. Published on June 25, 2012 as DOI: 10.1124/jpet.111.191239
This article has not been copyedited and formatted. The final version may differ from this version.

Fasudil modulates the expression of TNF-α and IL-1β and MPO activity

To test whether Fasudil modulates the inflammatory process through the regulation of secretion of pro-inflammatory cytokines, we analyzed spinal cord levels of TNF-α and IL-1 β (Fig. 5 G, H). A substantial increase in TNF-α and IL-1β production was found in spinal cord tissues samples collected from SCI mice 24 hours after SCI (Fig. 5 G, H). Spinal cord levels of TNF- α and IL-1β were significantly attenuated by the intraperitoneal injection of Fasudil (Fig. 5 G, H). Spinal cord sections were also taken at 24 h after SCI to determine the immunohistological staining for TNF-α and IL-1β expression. Spinal cord tissues obtained from Sham-operated mice did not stain for TNF-α and IL-1 β (Fig. 5 A, D and I). A substantial increase in TNF-α and IL-1β expression was found in inflammatory cells as well as in nuclei of Schwann cells in the white and gray matter of the spinal cord tissues collected from SCI mice 24 hours after SCI (Fig. 5 B, E and I). Fasudil treatment significantly reduced the degree of positive staining for these pro-inflammatory cytokines (Fig. 5 C, F and I) .

In this study, we also investigated the effect of the treatment of Fasudil on the infiltration of neutrophils by measuring tissue MPO activity. MPO activity was significantly elevated in the spinal cord at 24 h after injury in mice subjected to SCI when compared with Sham-operated mice (Fig. 5 L). In fasudil-treated mice, the MPO activity was significantly attenuated in comparison to that observed in SCI (Fig. 5 L).

Fasudil reduces the expression of MAP kinases

To investigate the cellular mechanisms by which treatment with Fasudil may attenuate the development of spinal cord injury, we also evaluated the activation of MAP kinases such as P-ERK by Western blot and P-JNK by immunohistochemistry and by Western blot. Spinal cord sections from sham-operated mice did not stain for P-JNK (Fig. 6 A, D) whereas spinal

cord sections obtained from SCI mice exhibited a positive staining for P-JNK (Fig. 6 B, D). Fasudil treatment reduced the degree of positive staining for P-JNK in the spinal cord of mice subjected to SCI (Fig. 6 C, D). In addition, in spinal cord tissue homogenates after SCI a significant increase in P-ERK and P-JNK expression was observed in SCI mice (Fig. 6 E, F). Treatment of mice with Fasudil significantly reduced P-ERK and P-JNK expression (Fig. 6 E, F).

Effect of Fasudil on ROK activity

Because Rho-kinase inhibits myosin phosphatase by phosphorylating its myosin-binding subunit, myosin phosphate target subunit-1 (MYPT1) (Sharpe and Hendry, 2003), we measured phosphorylated levels of MYPT1 in spinal cord tissues as a marker of Rho-kinase activity. Western blot analysis revealed that the levels of MYPT1 phosphorylation in spinal cord tissues were markedly increased in mice subjected to SCI indicating that Rho-kinase was activated after trauma. The increase in spinal cord tissues of MYPT1 phosphorylation was prevented by treatment with fasudil (Fig. 7).

Effects of Fasudil on nitrotyrosine and PAR formation

Spinal cord sections from sham-operated mice did not stain for nitrotyrosine and PAR (Fig. 8 A, D and G), whereas spinal cord sections obtained from SCI mice exhibited positive staining for nitrotyrosine and PAR (Fig. 8 B, E and G). The positive staining was mainly localized in inflammatory cells as well as in nuclei of Schwann cells in the white and gray matter of the spinal cord tissues. Fasudil treatment reduced the degree of positive staining for nitrotyrosine and PAR (Fig. 8 C, F and G) in the spinal cord.

JPET Fast Forward. Published on June 25, 2012 as DOI: 10.1124/jpet.111.191239
This article has not been copyedited and formatted. The final version may differ from this version.

Effects of Fasudil on FAS ligand expression

Immunohistological staining for FAS ligand in the spinal cord was also determined 24 h after injury. Spinal cord sections from sham-operated mice did not stain for FAS ligand (Fig. 9 A, G) whereas spinal cord sections obtained from SCI mice exhibited positive staining for FAS ligand mainly localized in inflammatory cells as well as in nuclei of Schwann cells (Fig. 9 B, G). Fasudil treatment reduced the degree of positive staining for FAS ligand in the spinal cord (Fig. 9 C, G).

Effects of Fasudil in the apoptosis in spinal cord after injury

To test whether spinal cord damage was associated to cell death by apoptosis, we also measured TUNEL-like staining in the perilesional spinal cord tissue. Almost no apoptotic cells were detected in the spinal cord from sham-operated mice (Fig. 9 D and H). At 24 h after the trauma, tissues from SCI mice demonstrated a marked appearance of dark brown apoptotic cells and intercellular apoptotic fragments (Fig. 9 E and H). In contrast, tissues obtained from mice treated with Fasudil treatment demonstrated no apoptotic cells or fragments (Fig. 9 F and H).

Western blot analysis and immunohistochemistry for Bax and Bcl-2

At 24 h after SCI, the appearance of proapoptic protein, Bax, in spinal cord homogenates was investigated by Western blot. Bax levels were appreciably increased in the spinal cord from mice subjected to SCI (Fig. 10 H). On the contrary, Fasudil treatment prevented the SCI-induced Bax expression (Fig. 10 H). By Western blot analysis were also analyzed Bcl-2 expression in homogenates from spinal cord of each mice. A basal level of Bcl-2 expression was detected in spinal cord from sham-operated mice (Fig. 10 I). Twenty-four hours after

SCI, the Bcl-2 expression was significantly reduced in spinal cord from SCI mice (Fig. 10 I). Treatment of mice with Fasudil significantly blunted the SCI-induced inhibition of anti-apoptotic protein expression (Fig. 10 I).

Moreover, samples of spinal cord tissue were taken at 24 h after SCI also to determine the immunohistological staining for Bax and Bcl-2. Spinal cord sections from sham-operated mice did not stain for Bax (Fig. 10 A, G) whereas spinal cord sections obtained from SCI mice exhibited a positive staining for Bax (Fig. 10 B, G). Fasudil treatment reduced the degree of positive staining for Bax in the spinal cord of mice subjected to SCI (Fig. 10 C, G). In addition, spinal cord sections from sham-operated mice demonstrated Bcl-2 positive staining (Fig. 10 D, G) while in SCI mice the staining significantly reduced (Fig. 10 E, G). Fasudil treatment attenuated the loss of positive staining for Bcl-2 in the spinal cord from SCI- subjected mice (Fig. 10 F, G).

JPET Fast Forward. Published on June 25, 2012 as DOI: 10.1124/jpet.111.191239
This article has not been copyedited and formatted. The final version may differ from this version.

Discussion

Spinal cord injury is a highly debilitating pathology. The pathological events following acute SCI are divided into two chronological phases (Tator and Fehlings, 1991). The traumatic mechanical injury to the spinal cord, that is incurred following blunt impact and compression, is called *"primary injury"*; it causes the death of a number of neurons that cannot be recovered and regenerated. The events that characterize this successive phase to mechanical injury are called *"secondary damage*." The secondary damage is determined by a large number of cellular, molecular, and biochemical cascades.

The Rho family of small GTPases is a group of 20–40–kd monomeric G proteins that can regulate a number of cellular biologic functions, including actin stress fiber formation, focal adhesion, motility, aggregation, proliferation, and transcription (Burridge and Wennerberg, 2004). Regulation of these cellular functions by Rho is mainly dependent on the activation of its downstream effector, Rho kinase (ROK) (Burridge and Wennerberg, 2004). It is also involved in the regulation of several aspects of innate immunity, including leukocyte chemotaxis, phagocytosis, and ROS formation (Riento and Ridley, 2003; Bokoch, 2005). Rho GTPases have been implicated in the modulation of NF-κB activation and T cell proliferation (Tharaux et al., 2003). It has also been reported that inhibition of Rho kinase suppresses NF-κB activation and IκB phosphorylation and degradation in peripheral blood mononuclear cells (PBMCs) from patients with Crohn's disease (Segain et al., 2003).

The aim of the present study was to determine the effect of Fasudil a ROK inhibitor, in the modulation of secondary injury associated with SCI. We show here that SCI resulted in edema and loss of myelin in lateral and dorsal funiculi. This histological damage was associated to the loss of motor function. In this study, we demonstrated that administration of fasudil inhibits the development of SCI through its effects on the NF-κB activation pathway and also, possibly, through other pathways (Okamoto et al., 2010).

JPET Fast Forward. Published on June 25, 2012 as DOI: 10.1124/jpet.111.191239
This article has not been copyedited and formatted. The final version may differ from this version.

In the study we report that SCI was associated with significant IκB-α degradation as well as increased nuclear expression of p65 in spinal cord tissue at 24 h after injury. Fasudil significantly reduced IκB-α degradation as well as the NF-κB translocation. A direct consequence of the inhibitory effect of fasudil on NF-κB activation is reduction of proinflammatory cytokines secretion (He et al., 2008). We have clearly confirmed a significant increase in TNF-α and IL-1β during SCI. On the contrary, no significant expression of TNF-α and IL-1β was observed in the spinal cord sections obtained from SCI-operated mice which received fasudil. A study in vitro also demonstrated that the treatment with fasudil or Y27632 decreased production of TNF–α, IL-1β, and IL-6 by synovial membrane cells, peripheral blood mononuclear cells, and fibroblast-like synoviocytes from patients with active rheumatoid arthritis (He et al., 2008).

IL-1β is produced in large amounts by infiltrating macrophages and neutrophils and is initially expressed in its proform and is only converted to a biologically active form following proteolytic cleavage by the protease caspase-1 (Thornberry et al., 1992). Caspase-1 is activated in the cytosol in a multiprotein scaffold termed the inflammasome (Martinon et al., 2002) which forms only in response to different danger signals (Miao et al., 2008). The best characterized inflammasome is the NLRP3 (also known as NALP3 and cryopyrin) inflammasome. It comprises the NLR protein NLRP3, the adapter ASC and pro-caspase-1 (Lamkanfi et al., 2009). Thus, caspase-1 activation is a central regulator of the innate immune defense. Recent work has indicated that the activation of Rho GTPases, in particular Rac1 and possibly Cdc42, might represent a novel type of signaling input that can activate caspase-1 signaling (Muller et al., 2010). In that regard, the treatment with a ROK inhibitor, fasudil, could be interfere with activation or assembly of the inflammasome but the mechanism is still unclear. Activation of Rho-A leads to stimulation of Rho kinase which can phosphorylate and subsequently inactivate the myosin light chain (MLC) phosphatase favoring actin-myosin

interaction and cell contraction (da Silva-Santos et al., 2009). Because Rho-kinase inhibits myosin phosphatase by phosphorylating its myosin-binding subunit, myosin phosphate target subunit-1 (MYPT1) (Sharpe and Hendry, 2003), we measured phosphorylated levels of MYPT1 in spinal cord tissues as a marker of Rho-kinase activity and we showed that spinal cord injury is associated with increases in ROK activity and fasudil treatment markedly attenuated ROK activity.

Several studies also showed that fasudil markedly reduced the endotoxin-induced increase of MPO activity, indicating an inhibitory effect of fasudil on leukocyte accumulation in endotoxemic liver injury (Thorlacius et al., 2006). Here, we report that SCI was associated with significant increase of neutrophil infiltration measured by MPO activity, while in fasudil-treated mice, the MPO activity was significantly attenuated in comparison to that observed in SCI.

The initiation of inflammatory responses in CNS is also related to activation of MAPKs, and their activation would be determinant for neuronal death or survival on certain occasions. Previous studies showed that the expression of activated ERK1/2 and p38 MAPK in microglia/macrophages may play a key role in production of CNS inflammatory cytokines and free radicals, such as NO (Choi et al., 2003). We confirm here that SCI leads to a substantial expression of P-ERK and P-JNK in the spinal cord tissues at 24 h after SCI, on the contrary the fasudil treatment decreases P-ERK and P-JNK expression in treated-mice. Chen et al., have also shown that fasudil effectively suppressed 5-HT-induced pulmonary artery smooth muscle cells (PASMC) proliferation and cell-cycle progression, which was associated with inhibition of JNK activation, ERK translocation to nucleus and subsequent c-fos and c-jun expression (Chen et al., 2009).

Among the reactive oxygen species, peroxynitrite ($ONOO^-$) is known to play an important role in local and systemic inflammatory response as well as neurodegenerative disease (Xu et

al., 2001). It is one of a number of toxic factors produced in the spinal cord tissues after SCI (Xu et al., 2001) likely contributes to secondary neuronal damage through pathways resulting from the chemical modification of cellular proteins and lipids. To probe the pathological contributions of $ONOO^-$ to secondary damage after SCI, we have used the appearance of nitrotyrosine staining in the inflamed tissue. We have observed that the immunoassaying of nitrotyrosine is reduced in SCI operated mice treated with fasudil when compared with SCI operated mice. A recent study also demonstrated that the administration of fasudil inhibited the activity of ROK in brain tissue and cultured microglia, and protected hippocampal neurons reducing the pro-inflammatory factors such as NO, IL-1β, IL-6 and TNF-α in a vivo model of hypoxia/reoxygenation (H/R) injury (Ding et al., 2011). Several lines of evidence clearly demonstrated that NO also plays a key role in regulating the expression of GFAP in astrocytes (Brahmachari et al., 2006). Although activated astrocytes secrete different neurotrophic factors for neuronal survival, it is believed that rapid and severe activation augments/ initiates an inflammatory response, leading to neuronal death and brain injury (Tani et al., 1996). Astrocytes react to various neurodegenerative insults rapidly, leading to vigorous astrogliosis (Eng et al., 1992). For this reason, in this study we have also evaluated by immunohistochemical analysis the expression of GFAP, a marker of astrocytic activation, and we have observed an high expression in SCI-subjected mice compared with fasudil-treated mice.

A novel pathway of inflammation associated to SCI, governed by the nuclear enzyme PARP has been proposed in relation to hydroxyl radical and peroxynitrite-induced DNA single strand breakage (Szabo and Dawson, 1998). Continuous or excessive activation of PARP produces extended chains of ADP-ribose (PAR) on nuclear proteins and results in a substantial depletion of intracellular NAD+ and subsequently ATP leading to cellular

dysfunction and ultimately, cell death (Chiarugi, 2002). We demonstrate here that fasudil reduced the increase of PARP activation in the spinal cord in animals subjected to SCI.

Apoptosis is an important mediator of secondary damage after SCI (Beattie et al., 2002). In an effort to prevent or diminish levels of apoptosis, we demonstrate that the treatment with fasudil attenuates the degree of apoptosis, measured by TUNEL detection kit, in the spinal cord after the damage. Wang et al., have also reported that fasudil, a Rho-kinase inhibitor, could attenuate Ang II–induced abdominal aortic aneurysm (AAA) formation by inhibiting vascular wall apoptosis and extracellular matrix proteolysis (Wang et al., 2005). A recent study also determined whether ROK inhibitor, fasudil, inhibited ischemic neuronal apoptosis through phosphatase and tensin homolog deleted on chromosome 10 (PTEN)/Akt/signal pathway in vivo (Wu et al., 2012). Here, we demonstrated that the treatment with fasudil reduced Bax expression, while on the contrary, Bcl-2 is expressed much more in mice treated with fasudil. Some authors have also shown that FAS and p75 receptors are expressed on oligodendrocytes, astrocytes and microglia in the spinal cord following SCI (Ackery et al., 2006). Therefore, FasL plays a central role in apoptosis induced by a variety of chemical and physical insults (Dosreis et al., 2004). In the present study, we found that fasudil treatment leads to a substantial reduction of FasL activation.

Finally, in this study we demonstrate that fasudil treatment significantly reduced the SCI-induced spinal cord tissues alteration as well as improve the motor function. The results of the present study enhance our understanding of the role of ROK activation in the pathophysiology of spinal cord cell and tissue injury following trauma, implying that inhibitors of the ROK such as fasudil, may be useful in the therapy of spinal cord injury and inflammation.

Acknowledgements

The authors would like to thank Carmelo La Spada for his excellent technical assistance during this study, Mrs Caterina Cutrona for secretarial assistance and Miss Valentina Malvagni for editorial assistance with the manuscript.

Autorship Contributions

Partecipated in research design: Salvatore Cuzzocrea, Emanuela Esposito

Conducted experiments: Daniela Impellizzeri, Emanuela Mazzon, Irene Paterniti

Performed data analysis: Salvatore Cuzzocrea, Emanuela Esposito

Wrote or contributed to the writing of manuscript: Daniela Impellizzeri, Salvatore Cuzzocrea

References

Abe K, Shimokawa H, Morikawa K, Uwatoku T, Oi K, Matsumoto Y, Hattori T, Nakashima Y, Kaibuchi K, Sueishi K and Takeshit A (2004) Long-term treatment with a Rho-kinase inhibitor improves monocrotaline-induced fatal pulmonary hypertension in rats. *Circ Res* **94**:385-393.

Ackery A, Robins S and Fehlings MG (2006) Inhibition of Fas-mediated apoptosis through administration of soluble Fas receptor improves functional outcome and reduces posttraumatic axonal degeneration after acute spinal cord injury. *J Neurotrauma* **23**:604-616.

Bao W, Hu E, Tao L, Boyce R, Mirabile R, Thudium DT, Ma XL, Willette RN and Yue TL (2004) Inhibition of Rho-kinase protects the heart against ischemia/reperfusion injury. *Cardiovasc Res* **61**:548-558.

Basso DM, Fisher LC, Anderson AJ, Jakeman LB, McTigue DM and Popovich PG (2006) Basso Mouse Scale for locomotion detects differences in recovery after spinal cord injury in five common mouse strains. *J Neurotrauma* **23**:635-659.

Beattie MS, Hermann GE, Rogers RC and Bresnahan JC (2002) Cell death in models of spinal cord injury. *Prog Brain Res* **137**:37-47.

Beattie MS, Li Q and Bresnahan JC (2000) Cell death and plasticity after experimental spinal cord injury. *Prog Brain Res* **128**:9-21.

Bethea JR, Castro M, Keane RW, Lee TT, Dietrich WD and Yezierski RP (1998) Traumatic spinal cord injury induces nuclear factor-kappaB activation. *J Neurosci* **18**:3251-3260.

Bokoch GM (2005) Regulation of innate immunity by Rho GTPases. *Trends Cell Biol* **15**:163-171.

Bourgier C, Haydont V, Milliat F, Francois A, Holler V, Lasser P, Bourhis J, Mathe D and Vozenin-Brotons MC (2005) Inhibition of Rho kinase modulates radiation induced fibrogenic phenotype in intestinal smooth muscle cells through alteration of the cytoskeleton and connective tissue growth factor expression. *Gut* **54**:336-343.

Bowie A and O'Neill LA (2000) Oxidative stress and nuclear factor-kappaB activation: a reassessment of the evidence in the light of recent discoveries. *Biochem Pharmacol* **59**:13-23.

Brahmachari S, Fung YK and Pahan K (2006) Induction of glial fibrillary acidic protein expression in astrocytes by nitric oxide. *J Neurosci* **26**:4930-4939.

Burridge K and Wennerberg K (2004) Rho and Rac take center stage. *Cell* **116**:167-179.

Chen CC, Chow MP, Huang WC, Lin YC and Chang YJ (2004) Flavonoids inhibit tumor necrosis factor-alpha-induced up-regulation of intercellular adhesion molecule-1 (ICAM-1) in respiratory epithelial cells through activator protein-1 and nuclear factor-kappaB: structure-activity relationships. *Mol Pharmacol* **66**:683-693.

Chen XY, Dun JN, Miao QF and Zhang YJ (2009) Fasudil hydrochloride hydrate, a Rho-kinase inhibitor, suppresses 5-hydroxytryptamine-induced pulmonary artery smooth muscle cell proliferation via JNK and ERK1/2 pathway. *Pharmacology* **83**:67-79.

Chiarugi A (2002) Poly(ADP-ribose) polymerase: killer or conspirator? The 'suicide hypothesis' revisited. *Trends Pharmacol Sci* **23**:122-129.

Choi SH, Joe EH, Kim SU and Jin BK (2003) Thrombin-induced microglial activation produces degeneration of nigral dopaminergic neurons in vivo. *J Neurosci* **23**:5877-5886.

da Silva-Santos JE, Chiao CW, Leite R and Webb RC (2009) The Rho-A/Rho-kinase pathway is up-regulated but remains inhibited by cyclic guanosine monophosphate-

dependent mechanisms during endotoxemia in small mesenteric arteries. *Crit Care Med* **37**:1716-1723.

Ding J, Li QY, Wang X, Sun CH, Lu CZ and Xiao BG (2011) Fasudil protects hippocampal neurons against hypoxia-reoxygenation injury by suppressing microglial inflammatory responses in mice. *J Neurochem* **114**:1619-1629.

Ding RY, Zhao DM, Zhang ZD, Guo RX and Ma XC (2011) Pretreatment of rho kinase inhibitor inhibits systemic inflammation and prevents endotoxin-induced acute lung injury in mice. *J Surg Res* **171**:e209-214.

Dosreis GA, Borges VM and Zin WA (2004) The central role of Fas-ligand cell signaling in inflammatory lung diseases. *J Cell Mol Med* **8**:285-293.

Dostert C, Guarda G, Romero JF, Menu P, Gross O, Tardivel A, Suva ML, Stehle JC, Kopf M, Stamenkovic I, Corradin G and Tschopp J (2009) Malarial hemozoin is a Nalp3 inflammasome activating danger signal. *PLoS One* **4**:e6510.

Eng LF and Ghirnikar RS (1994) GFAP and astrogliosis. *Brain Pathol* **4**:229-237.

Eng LF, Yu AC and Lee YL (1992) Astrocytic response to injury. *Prog Brain Res* **94**:353-365.

Hausmann ON (2003) Post-traumatic inflammation following spinal cord injury. *Spinal Cord* **41**:369-378.

He Y, Xu H, Liang L, Zhan Z, Yang X, Yu X, Ye Y and Sun L (2008) Antiinflammatory effect of Rho kinase blockade via inhibition of NF-kappaB activation in rheumatoid arthritis. *Arthritis Rheum* **58**:3366-3376.

Lamkanfi M, Malireddi RK and Kanneganti TD (2009) Fungal zymosan and mannan activate the cryopyrin inflammasome. *J Biol Chem* **284**:20574-20581.

Li JM, Gall NP, Grieve DJ, Chen M and Shah AM (2002) Activation of NADPH oxidase during progression of cardiac hypertrophy to failure. *Hypertension* **40**:477-484.

Ma Z, Zhang J, Du R, Ji E and Chu L (2011) Rho Kinase Inhibition by Fasudil Has Anti-inflammatory Effects in Hypercholesterolemic Rats. *Biol Pharm Bull* **34**:1684-1689.

Martinon F, Burns K and Tschopp J (2002) The inflammasome: a molecular platform triggering activation of inflammatory caspases and processing of proIL-beta. *Mol Cell* **10**:417-426.

Miao EA, Ernst RK, Dors M, Mao DP and Aderem A (2008) Pseudomonas aeruginosa activates caspase 1 through Ipaf. *Proc Natl Acad Sci U S A* **105**:2562-2567.

Mullane K (1989) Neutrophil-platelet interactions and post-ischemic myocardial injury. *Prog Clin Biol Res* **301**:39-51.

Muller AJ, Hoffmann C and Hardt WD (2010) Caspase-1 activation via Rho GTPases: a common theme in mucosal infections? *PLoS Pathog* **6**:e1000795.

Nobunaga AI, Go BK and Karunas RB (1999) Recent demographic and injury trends in people served by the Model Spinal Cord Injury Care Systems. *Arch Phys Med Rehabil* **80**:1372-1382.

Okamoto H, Yoshio T, Kaneko H and Yamanaka H (2010) Inhibition of NF-kappaB signaling by fasudil as a potential therapeutic strategy for rheumatoid arthritis. *Arthritis Rheum* **62**:82-92.

Riento K and Ridley AJ (2003) Rocks: multifunctional kinases in cell behaviour. *Nat Rev Mol Cell Biol* **4**:446-456.

Rivlin AS and Tator CH (1978) Effect of duration of acute spinal cord compression in a new acute cord injury model in the rat. *Surg Neurol* **10**:38-43.

Sato T, Asamitsu K, Yang JP, Takahashi N, Tetsuka T, Yoneyama A, Kanagawa A and Okamoto T (1998) Inhibition of human immunodeficiency virus type 1 replication by a bioavailable serine/threonine kinase inhibitor, fasudil hydrochloride. *AIDS Res Hum Retroviruses* **14**:293-298.

Satoh S, Utsunomiya T, Tsurui K, Kobayashi T, Ikegaki I, Sasaki Y and Asano T (2001) Pharmacological profile of hydroxy fasudil as a selective rho kinase inhibitor on ischemic brain damage. *Life Sci* **69**:1441-1453.

Seasholtz TM and Brown JH (2004) RHO SIGNALING in vascular diseases. *Mol Interv* **4**:348-357.

Segain JP, Raingeard de la Bletiere D, Sauzeau V, Bourreille A, Hilaret G, Cario-Toumaniantz C, Pacaud P, Galmiche JP and Loirand G (2003) Rho kinase blockade prevents inflammation via nuclear factor kappa B inhibition: evidence in Crohn's disease and experimental colitis. *Gastroenterology* **124**:1180-1187.

Sharpe CC and Hendry BM (2003) Signaling: focus on Rho in renal disease. *J Am Soc Nephrol* **14**:261-264.

Shibuya M, Suzuki Y, Sugita K, Saito I, Sasaki T, Takakura K, Nagata I, Kikuchi H, Takemae T, Hidaka H and et al. (1992) Effect of AT877 on cerebral vasospasm after aneurysmal subarachnoid hemorrhage. Results of a prospective placebo-controlled double-blind trial. *J Neurosurg* **76**:571-577.

Shiotani S, Shimada M, Suehiro T, Soejima Y, Yosizumi T, Shimokawa H and Maehara Y (2004) Involvement of Rho-kinase in cold ischemia-reperfusion injury after liver transplantation in rats. *Transplantation* **78**:375-382.

Sirin BH, Ortac R, Cerrahoglu M, Saribulbul O, Baltalarli A, Celebisoy N, Iskesen I and Rendeci O (2002) Ischaemic preconditioning reduces spinal cord injury in transient ischaemia. *Acta Cardiol* **57**:279-285.

Stover SL and Fine PR (1987) The epidemiology and economics of spinal cord injury. *Paraplegia* **25**:225-228.

Streit WJ, Semple-Rowland SL, Hurley SD, Miller RC, Popovich PG and Stokes BT (1998) Cytokine mRNA profiles in contused spinal cord and axotomized facial nucleus suggest a beneficial role for inflammation and gliosis. *Exp Neurol* **152**:74-87.

Szabo C and Dawson VL (1998) Role of poly (ADP-ribose) synthetase in inflammation and ischaemia-reperfusion. *Trends Pharmacol Sci* **19**:287-298.

Tani M, Glabinski AR, Tuohy VK, Stoler MH, Estes ML and Ransohoff RM (1996) In situ hybridization analysis of glial fibrillary acidic protein mRNA reveals evidence of biphasic astrocyte activation during acute experimental autoimmune encephalomyelitis. *Am J Pathol* **148**:889-896.

Tator CH and Fehlings MG (1991) Review of the secondary injury theory of acute spinal cord trauma with emphasis on vascular mechanisms. *J Neurosurg* **75**:15-26.

Tharaux PL, Bukoski RC, Rocha PN, Crowley SD, Ruiz P, Nataraj C, Howell DN, Kaibuchi K, Spurney RF and Coffman TM (2003) Rho kinase promotes alloimmune responses by regulating the proliferation and structure of T cells. *J Immunol* **171**:96-105.

Thorlacius K, Slotta JE, Laschke MW, Wang Y, Menger MD, Jeppsson B and Thorlacius H (2006) Protective effect of fasudil, a Rho-kinase inhibitor, on chemokine expression, leukocyte recruitment, and hepatocellular apoptosis in septic liver injury. *J Leukoc Biol* **79**:923-931.

Thornberry NA, Bull HG, Calaycay JR, Chapman KT, Howard AD, Kostura MJ, Miller DK, Molineaux SM, Weidner JR, Aunins J and et al. (1992) A novel heterodimeric cysteine protease is required for interleukin-1 beta processing in monocytes. *Nature* **356**:768-774.

Wang N, Guan P, Zhang JP, Chang YZ, Gu LJ, Hao FK, Shi ZH, Wang FY and Chu L (2011) Preventive effects of fasudil on adriamycin-induced cardiomyopathy: Possible involvement of inhibition of RhoA/ROCK pathway. *Food Chem Toxicol* **49**:2975-82.

Wang YX, Martin-McNulty B, da Cunha V, Vincelette J, Lu X, Feng Q, Halks-Miller M, Mahmoudi M, Schroeder M, Subramanyam B, Tseng JL, Deng GD, Schirm S, Johns A, Kauser K, Dole WP and Light DR (2005) Fasudil, a Rho-kinase inhibitor, attenuates angiotensin II-induced abdominal aortic aneurysm in apolipoprotein E-deficient mice by inhibiting apoptosis and proteolysis. *Circulation* **111**:2219-2226.

Wu J, Li J, Hu H, Liu P, Fang Y and Wu D (2012) Rho-Kinase Inhibitor, Fasudil, Prevents Neuronal Apoptosis via the Akt Activation and PTEN Inactivation in the Ischemic Penumbra of Rat Brain. *Cell Mol Neurobiol*.

Xu J, Kim GM, Chen S, Yan P, Ahmed SH, Ku G, Beckman JS, Xu XM and Hsu CY (2001) iNOS and nitrotyrosine expression after spinal cord injury. *J Neurotrauma* **18**:523-532.

JPET Fast Forward. Published on June 25, 2012 as DOI: 10.1124/jpet.111.191239
This article has not been copyedited and formatted. The final version may differ from this version.

Figure legends

Fig. 1: Effect of fasudil treatment on histological alterations of the spinal cord tissue 24 h after injury. A significant damage to the spinal cord, from SCI operated mice at the perilesional area, was assessed by the presence of edema as well as alteration of the white matter 24 h after injury **(B, B1).** Notably, a significant protection from the SCI was observed in the tissue collected from fasudil treated mice **(C, C1)** when compared with sham-operated mice **(A, A1).** The histological score was made by an independent observer. wm: White matter; gm: gray matter. This figure is representative of at least 3 experiments performed on different experimental days on the tissues section collected from all the animals in each group. Values shown are mean ± s.e. mean of 10 mice for each group. ***P*<0.01 vs. Sham °*P*<0.01 vs. *SCI* **(D).**

The motor function of mice subjected to compression trauma was assessed once a day for 10 days after injury. Recovery from motor disturbance was graded using the Basso Mouse Scale (Basso et al., 2006). Treatment with fasudil reduces the motor disturbance after SCI. Values shown are mean ± s.e. mean of 10 mice for each group. ***P*<0.01 vs. *SCI* **(E).** wm: white matter; gm: gray matter; ND: Not detectable.

Fig. 2. Effect of fasudil on GFAP expression. Spinal cord sections from sham-operated mice did not stain for GFAP **(A)** whereas SCI caused, at 24 h, an increase in GFAP expression **(B)**. Fasudil treatment reduced the degree of positive staining for GFAP in the spinal cord **(C)**. Densitometry analysis of immunocytochemistry photographs (n=5 photos from each sample collected from all mice in each experimental group) for GFAP **(D)** from spinal cord tissues was assessed. The assay was carried out by using Optilab Graftek software on a Macintosh personal computer (CPU G3-266). Data are expressed as % of total tissue area. This figure is

JPET Fast Forward. Published on June 25, 2012 as DOI: 10.1124/jpet.111.191239
This article has not been copyedited and formatted. The final version may differ from this version.

representative of at least 3 experiments performed on different experimental days on the tissues section collected from all the animals in each group. ***P*<0.01 vs. Sham; °*P*<0.01 vs. *SCI*+vehicle. wm: white matter; gm: gray matter; ND: Not detectable.

Fig. 3. Western blot analysis for IκB-α and NF-κB p65. A basal level of IκB-α was also detected in the spinal cord from sham-operated animals **(A)** whereas IκB-α levels were substantially reduced in SCI mice **(A).** Fasudil treatment prevented the SCI-induced IκB-α degradation **(A)**. In addition, SCI caused a significant increase in nuclear NF-κB p65 **(B)** compared to the sham-operated mice **(B).** Fasudil treatment significantly reduced NF-κB p65 levels as shown in figure **(B)**. β-actin was used as internal control. The relative expression of the protein bands was standardized for densitometric analysis to β-actin levels, and reported in fig are expressed as mean ± s.e.m. from n=5/6 spinal cord for each group. ***P*<0.01 vs. Sham; °*P*<0.01 vs *SCI*+vehicle. wm: white matter; gm: gray matter; ND: Not detectable.

Fig. 4. Effect of Fasudil on caspase 1 and NLRP3 expression. Representative western blots showing no significant caspase 1 and NLRP3 expression in spinal cord tissues obtained from sham-treated animals **(A, B)**. A significant increase in caspase 1 and NLRP3 **(A, B)** was observed in the spinal cord from mice subjected to SCI. On the contrary, fasudil treatment prevented the SCI-induced **(A, B)** expression of these proteins. Moreover, The relative expression of the protein bands was standardized for densitometric analysis to β-actin levels, and reported in figures **(A)** and **(B).** ***P*<0.01 vs. Sham; °*P*<0.01 vs. *SCI*+vehicle. wm: white matter; gm: gray matter; ND: Not detectable.

JPET Fast Forward. Published on June 25, 2012 as DOI: 10.1124/jpet.111.191239
This article has not been copyedited and formatted. The final version may differ from this version.

Fig. 5. Effects of fasudil on TNF-α and IL-1β expression and MPO activity. A substantial increase in TNF-α **(B)** and IL- 1β **(E)** expression was found in inflammatory cells, in nuclei of Schwann cells in wm and gm of the spinal cord tissues from SCI mice at 24 hours after SCI in comparison to sham groups **(A, D).** Spinal cord levels of TNF-α **(C)** and IL- 1β **(F)** were significantly attenuated in fasudil treated mice. In addition, a substantial increase in TNF-α **(G)** and IL-1β **(H)** production was found in spinal cord tissue collected from SCI mice at 24 h. Spinal cord levels of TNF-α and IL-1β were significantly attenuated by fasudil treatment **(G, H).**

Densitometry analysis of immunocytochemistry photographs (n=5 photos from each sample collected from all mice in each experimental group) for TNF-α and IL-1β **(I)** from spinal cord tissues was assessed. The assay was carried out by using Optilab Graftek software on a Macintosh personal computer (CPU G3-266). Data are expressed as % of total tissue area. This figure is representative of at least 3 experiments performed on different experimental days on the tissues section collected from all the animals in each group. ***P*<0.01 vs. Sham; °*P*<0.01 vs *SCI*+vehicle.

Following the injury, MPO activity in spinal cord from *SCI* mice was significantly increased at 24 h after the damage in comparison to sham groups **(L).** Treatment i.p. fasudil significantly attenuated neutrophil infiltration. Data are means ± s.e. means of 10 mice for each group. ***P*<0.01 vs. Sham; °*P*<0.01 vs *SCI*+vehicle. wm: white matter; gm: gray matter; ND: Not detectable.

Fig. 6. Effect of fasudil on phospho-JNK and P-ERK expression. SCI caused a positive staining for P-JNK at 24 h after trauma **(B).** The treatment with fasudil significantly reduced the degree of positive staining for P-JNK **(C).** Spinal cord sections from sham-operated mice

JPET Fast Forward. Published on June 25, 2012 as DOI: 10.1124/jpet.111.191239
This article has not been copyedited and formatted. The final version may differ from this version.

did not stain for P-JNK **(A).** Densitometry analysis of immunocytochemistry photographs (n=5 photos from each sample collected from all mice in each experimental group) for JNK **(D)** from spinal cord tissues was assessed. The assay was carried out by using Optilab Graftek software on a Macintosh personal computer (CPU G3-266). Data are expressed as % of total tissue area. This figure is representative of at least 3 experiments performed on different experimental days on the tissues section collected from all the animals in each group. **P*<0.01 vs. Sham; °*P*<0.01 vs. *SCI*+vehicle.

In addition, representative western blots showing no significant phospho-JNK and P-ERK expression in spinal cord tissues obtained from sham-treated animals **(E, F)**. A significant increase in phospho-JNK and P-ERK **(E, F)** was observed in the spinal cord from mice subjected to SCI. On the contrary, fasudil treatment prevented the SCI-induced **(E, F)** expression of these proteins. Moreover, The relative expression of the protein bands was standardized for densitometric analysis to β-actin levels, and reported in figures **(E)** and **(F).** ***P*<0.01 vs. Sham; °*P*<0.01 vs. *SCI*+vehicle. wm: white matter; gm: gray matter; ND: Not detectable.

Fig. 7. Effect of Fasudil on MYPT-1 phosphorylation (ROK activity). ROK activity was measured by phosphorylation of MYPT-1. No increase of MYPT-1 phosphorylation was observed in sham animals. Spinal cord phosphorylated levels of MYPT-1 were significantly increased in SCI subjected mice. Treatment with fasudil attenuated SCI-induced MYPT-1 phosphorylation. β-actin was used as internal control. The relative expression of the protein bands was standardized for densitometric analysis to β-actin levels, and reported in fig are expressed as mean ± s.e.m. from n=5/6 spinal cord for each group. ***P*<0.01 vs. Sham; °*P*<0.01 vs *SCI*+vehicle. wm: white matter; gm: gray matter; ND: Not detectable.

JPET Fast Forward. Published on June 25, 2012 as DOI: 10.1124/jpet.111.191239
This article has not been copyedited and formatted. The final version may differ from this version.

Fig. 8. Effects of fasudil on nitrotyrosine and PAR formation. Spinal cord sections from sham-operated mice did not stain for nitrotyrosine **(A)**. Sections obtained from vehicle-treated animals after SCI demonstrate positive staining for nitrotyrosine mainly localized in inflammatory cells, in nuclei of Schwann cells in the white and gray matter **(B)**. Fasudil treatment (10 mg/kg 1 and 6 h after SCI induction) reduced the degree of positive staining for nitrotyrosine **(C)** in the spinal cord. In addition, immunohistochemistry for PAR, an indicator of in vivo PARP activation, revealed the occurrence of positive staining for PAR localized in nuclei of Schwann cells in wm and gm of the spinal cord tissues from SCI mice **(E).** Spinal cord sections from sham-operated mice did not also stain for PAR **(D)**. Fasudil treatment reduced the degree of positive staining for PAR **(F)** in the spinal cord. Densitometry analysis of immunocytochemistry photographs (n=5 photos from each sample collected from all mice in each experimental group) for nitrotyrosine and PAR **(G)** from spinal cord tissues was assessed. The assay was carried out by using Optilab Graftek software on a Macintosh personal computer (CPU G3-266). Data are expressed as % of total tissue area. This figure is representative of at least 3 experiments performed on different experimental days on the tissues section collected from all the animals in each group. $^{**}P<0.01$ vs. Sham; $^{\circ}P<0.01$ vs *SCI*+vehicle. wm: white matter; gm: gray matter; ND: Not detectable.

Fig. 9. Effect of fasudil on FAS-ligand expression and on TUNEL-like staining in the perilesional spinal cord tissue. Spinal cord sections were processed at 24 h after SCI to determine the immunohistological staining for Fas-ligand and TUNEL staining. Spinal cord sections from sham-operated mice did not stain for FAS ligand **(A)** whereas a substantial increase in Fas-ligand expression was found in inflammatory cells, in nuclei of Schwann cells in wm and gm of the spinal cord tissues from SCI mice at 24 hours after SCI **(B)**. Spinal cord levels of Fas-ligand were significantly attenuated in fasudil treated mice in comparison to SCI

JPET Fast Forward. Published on June 25, 2012 as DOI: 10.1124/jpet.111.191239
This article has not been copyedited and formatted. The final version may differ from this version.

animals **(C)**. Densitometry analysis of immunocytochemistry photographs (n=5 photos from each sample collected from all mice in each experimental group) for Fas-ligand **(G)** from spinal cord tissues was assessed. The assay was carried out by using Optilab Graftek software on a Macintosh personal computer (CPU G3-266). Data are expressed as % of total tissue area. This figure is representative of at least 3 experiments performed on different experimental days on the tissues section collected from all the animals in each group. ***P*<0.01 vs. Sham; °*P*<0.01 vs *SCI*+vehicle.

Moreover, almost no apoptotic cells were detected in the spinal cord from sham-operated mice **(D).** At 24 h after the trauma, SCI mice demonstrated a marked appearance of dark brown apoptotic cells and intercellular apoptotic fragments **(E)**. In contrast, tissues obtained from mice treated with fasudil demonstrated no apoptotic cells or fragments **(F)**. The number of TUNEL positive cells/high-power field was counted in 5 to 10 fields for each coded slide **(H)**. Figure is representative of at least 3 experiments performed on different experimental days on the tissues section collected from all the animals in each group. ***P*<0.01 vs. Sham; °*P*<0.01 vs *SCI*+vehicle. wm: white matter; gm: gray matter; ND: Not detectable.

Fig. 10. Effect of fasudil on expression of Bax and Bcl-2. Spinal cord sections from sham-operated mice did not stain for Bax **(A)** whereas SCI caused, at 24 h, an increase in Bax expression **(B)**. Fasudil treatment reduced the degree of positive staining for Bax in the spinal cord **(C)**. On the contrary, positive staining for Bcl-2 was observed in the spinal cord tissues from sham-operated mice **(D)** while the staining was significantly reduced in SCI mice **(E)**. Fasudil treatment attenuated the loss of positive staining for Bcl-2 in the spinal cord from SCI-subjected mice **(F)**. Densitometry analysis of immunocytochemistry photographs (n=5 photos from each sample collected from all mice in each experimental group) for Bax and for

JPET Fast Forward. Published on June 25, 2012 as DOI: 10.1124/jpet.111.191239
This article has not been copyedited and formatted. The final version may differ from this version.

Bcl-2 **(G)** from spinal cord tissues was assessed. The assay was carried out by using Optilab Graftek software on a Macintosh personal computer (CPU G3-266). Data are expressed as % of total tissue area. This figure is representative of at least 3 experiments performed on different experimental days on the tissues section collected from all the animals in each group. ***P*<0.01 vs. Sham; °*P*<0.01 vs. *SCI*+vehicle. In addition, representative Western blots showing no significant Bax expression in spinal cord tissues obtained from sham-treated animals **(H).** Bax levels were appreciably increased in the spinal cord from SCI mice **(H)**. On the contrary, fasudil prevented the SCI-induced Bax expression **(H).** Moreover, a basal level of Bcl-2 expression was detected in spinal cord from sham-operated mice **(I)**. Twenty-four hours after SCI, Bcl-2 expression was significantly reduced in spinal cord from SCI mice **(I)**. Fasudil treatment significantly reduced the SCI-induced inhibition of Bcl-2 expression **(I)**. Moreover, The relative expression of the protein bands was standardized for densitometric analysis to β-actin levels, and reported in figures **(H)** and **(I).** ***P*<0.01 vs. Sham; °*P*<0.01 vs. *SCI*+vehicle. wm: white matter; gm: gray matter; ND: Not detectable.

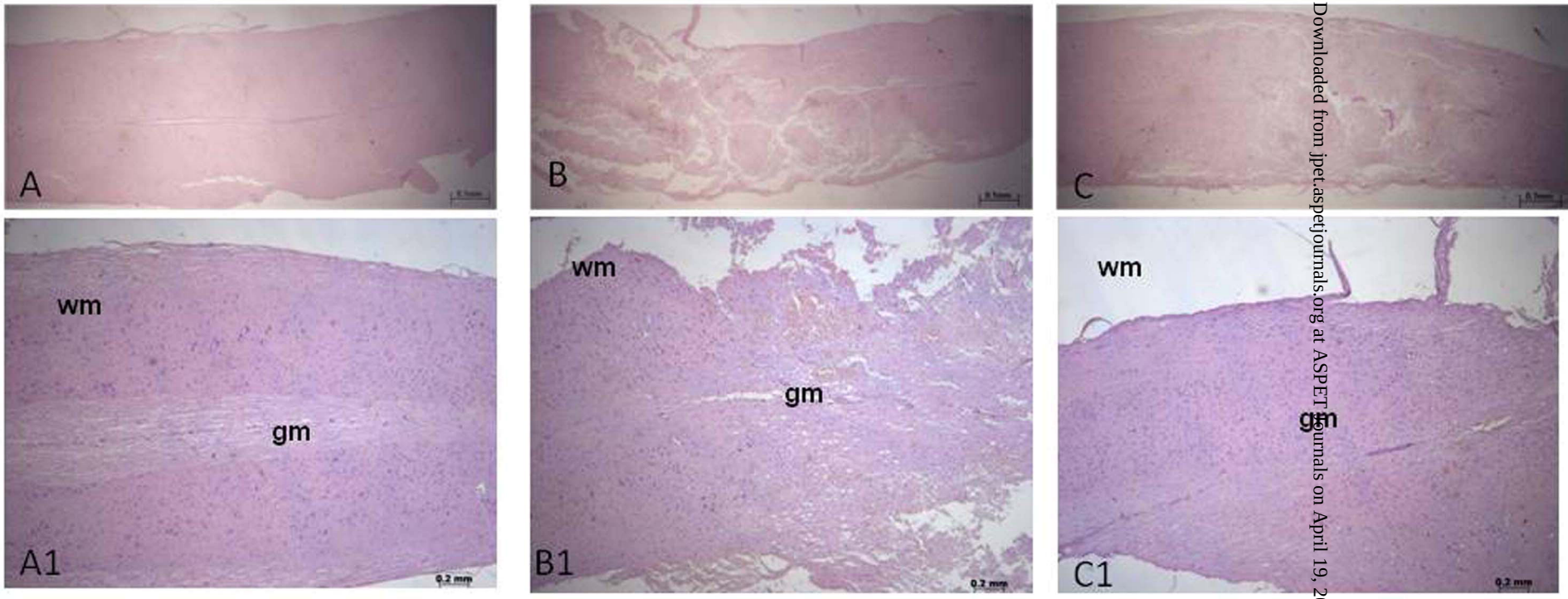

Figure 1

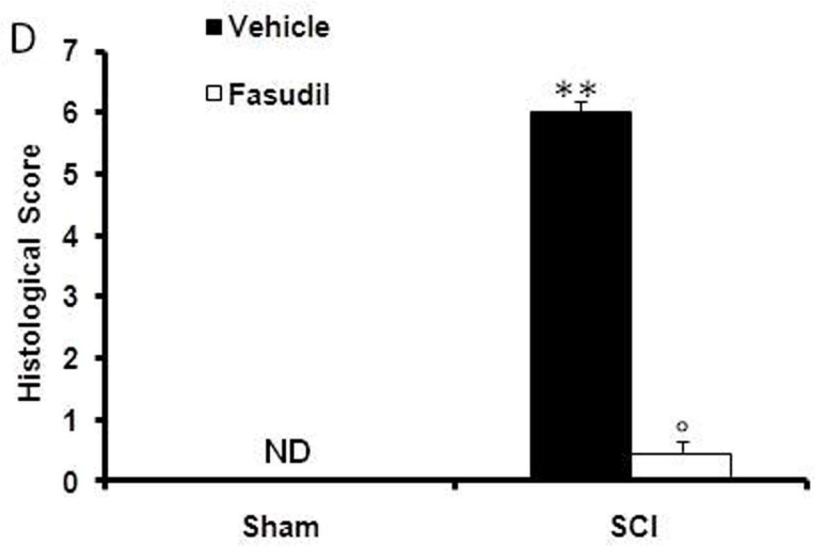

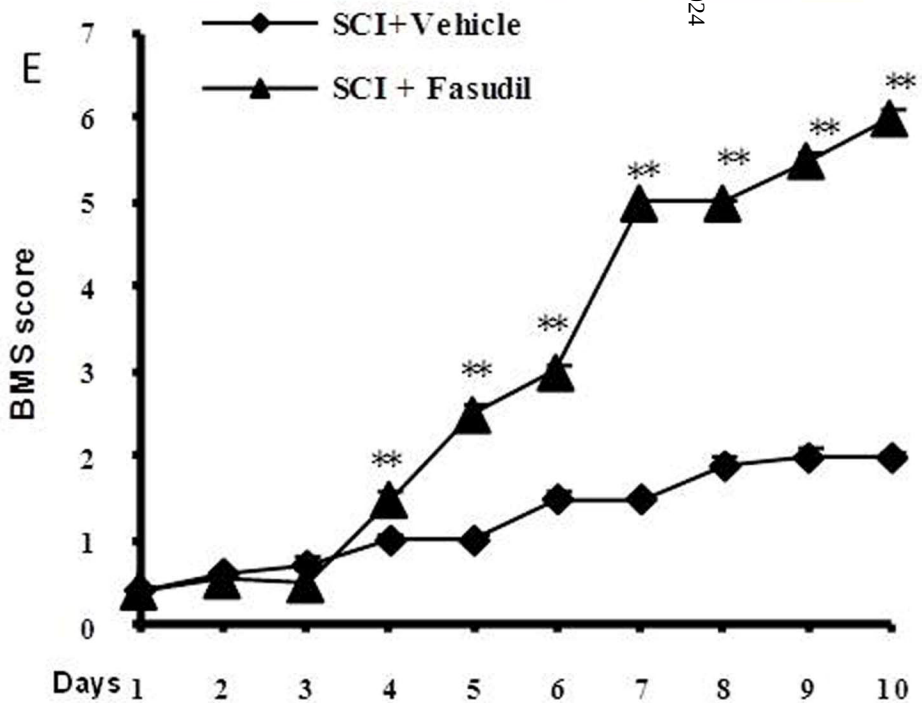

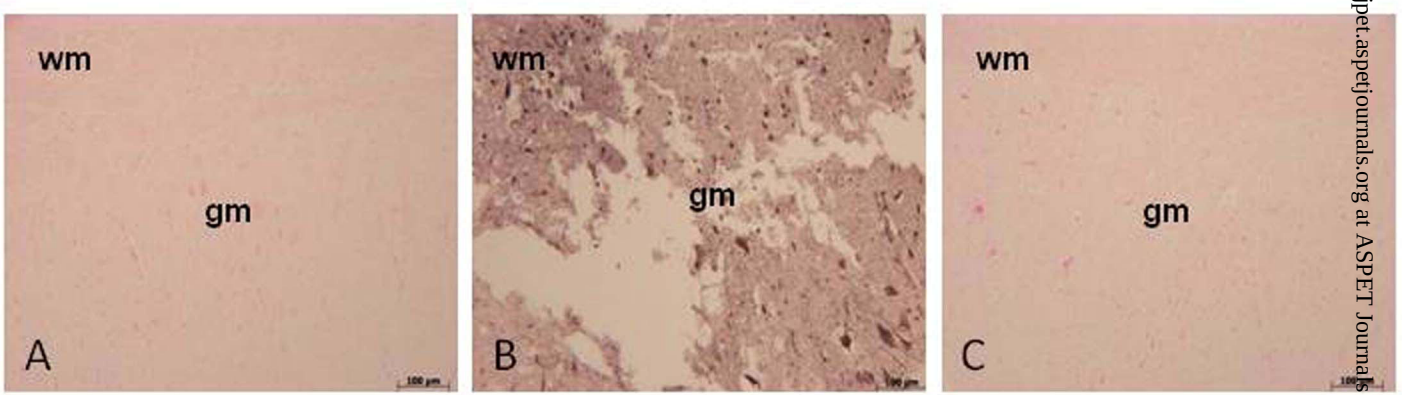

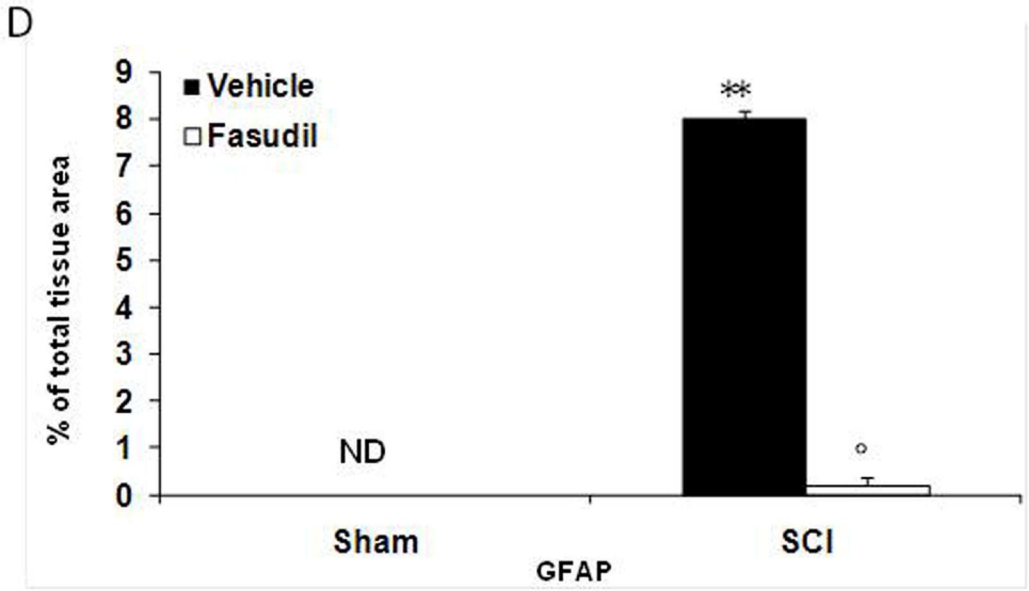

Figure 2

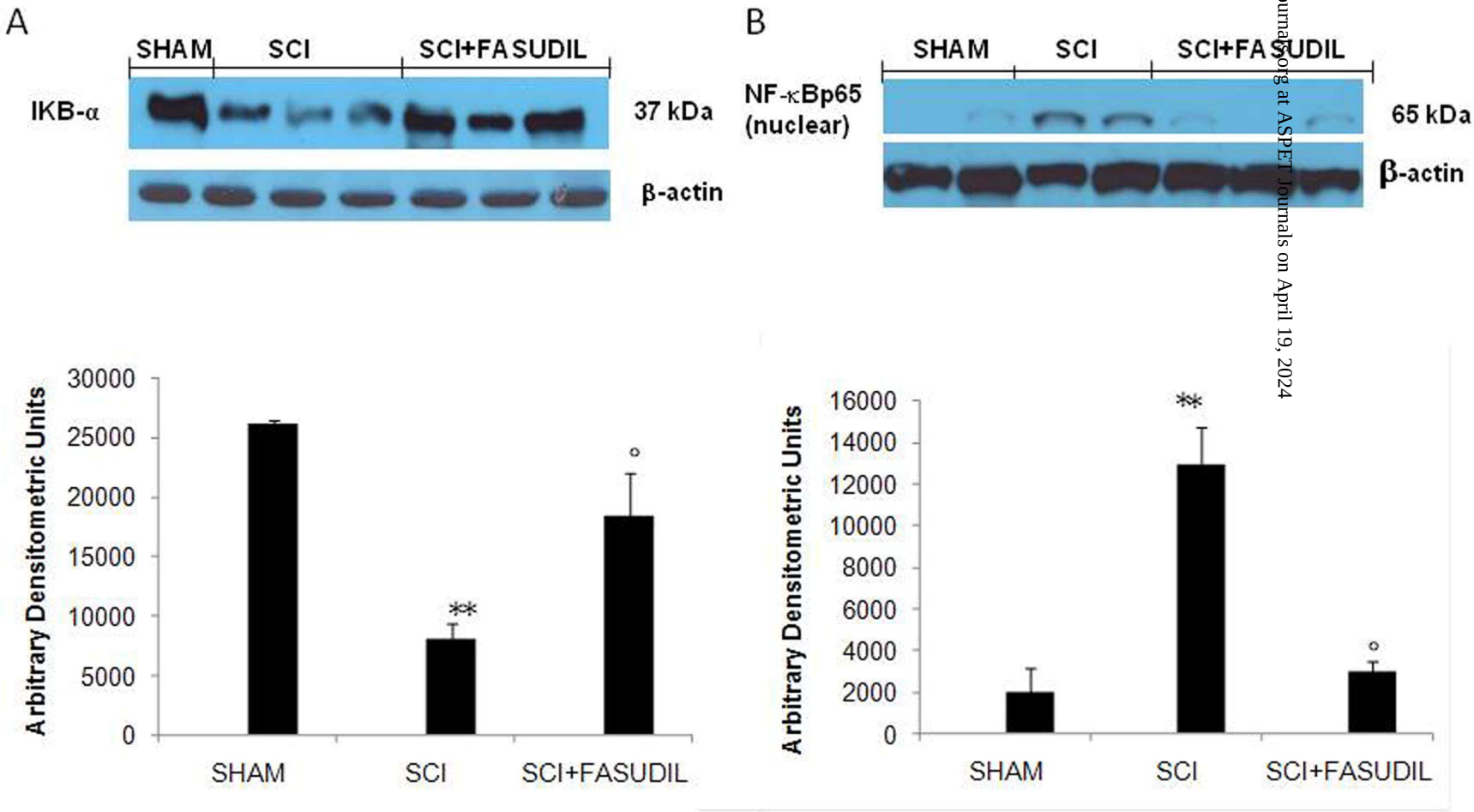

Figure 3

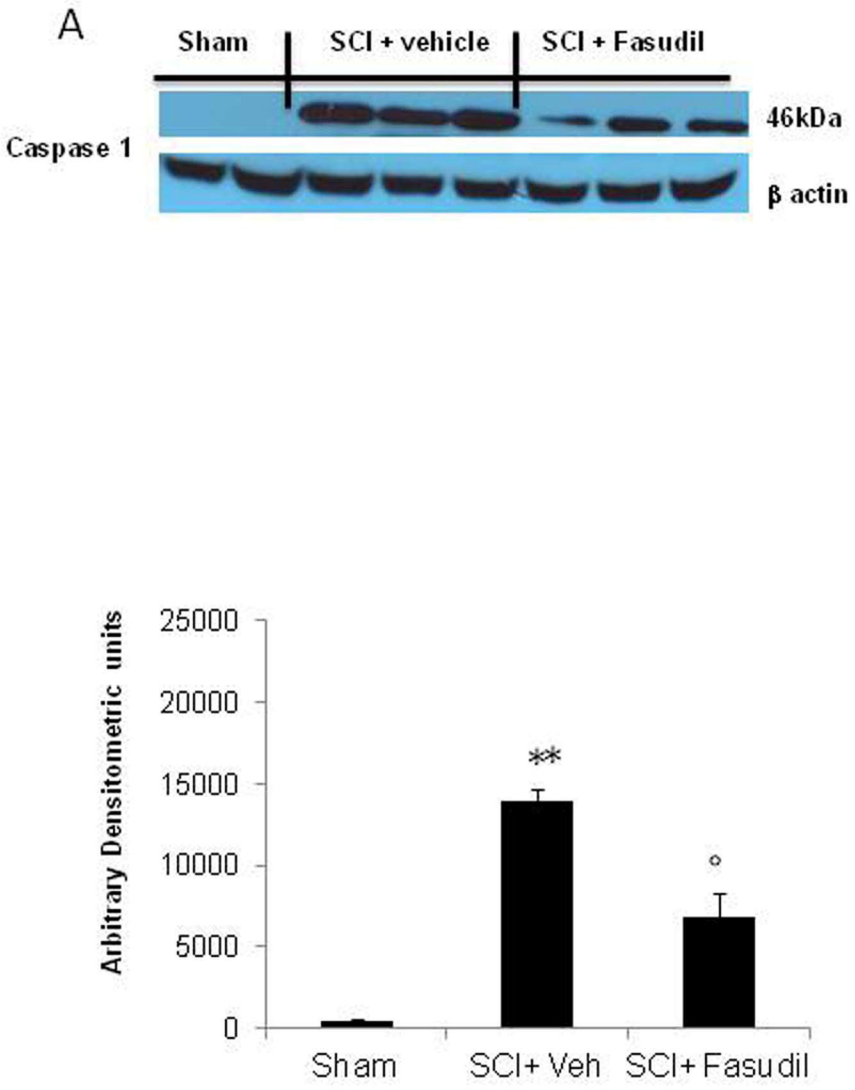

Figure 4

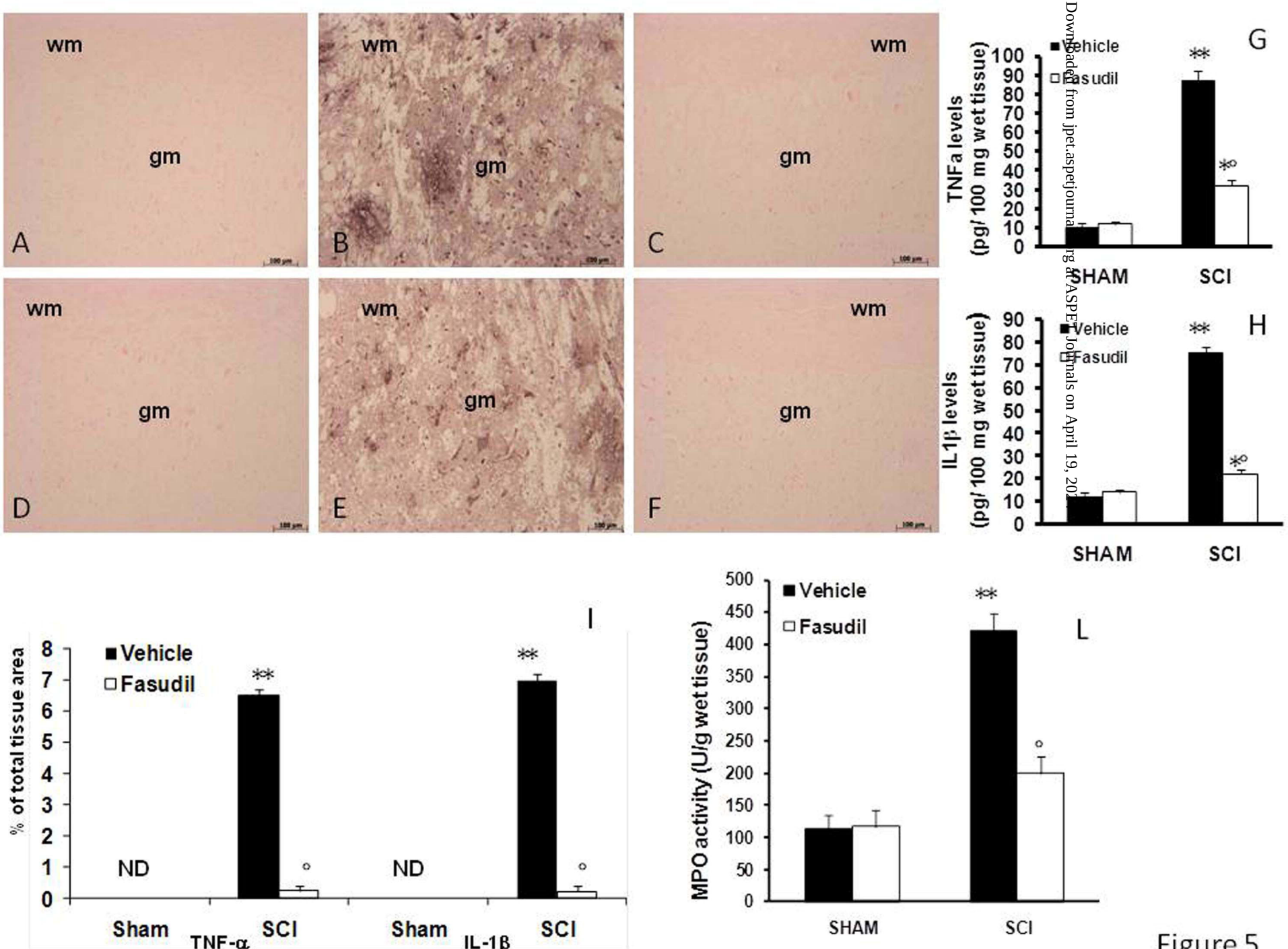

Figure 5

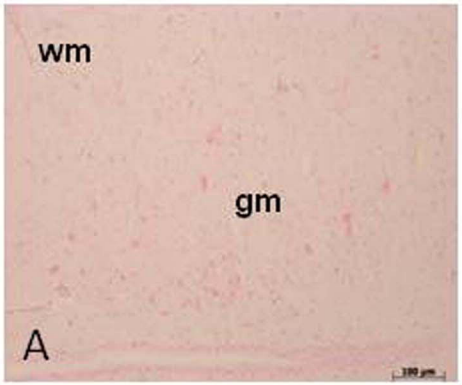

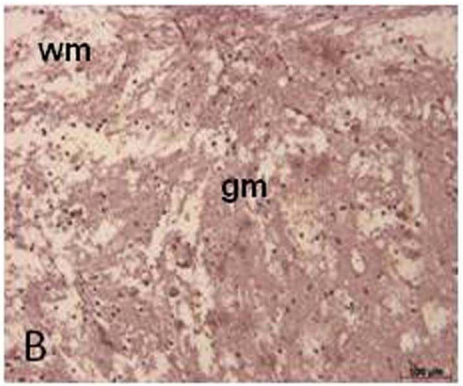

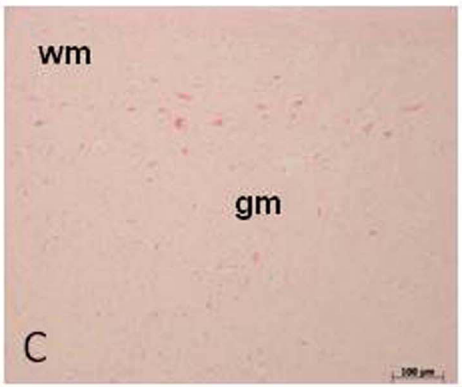

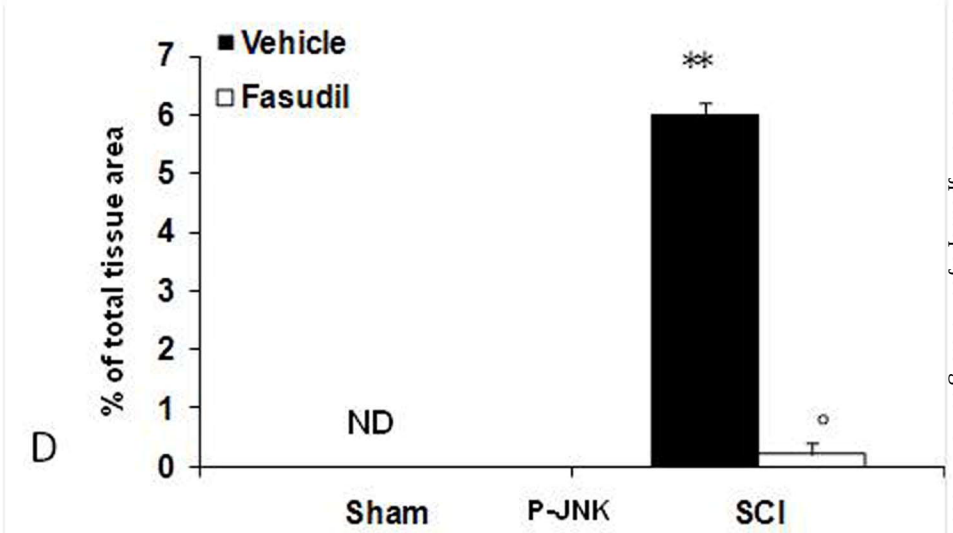

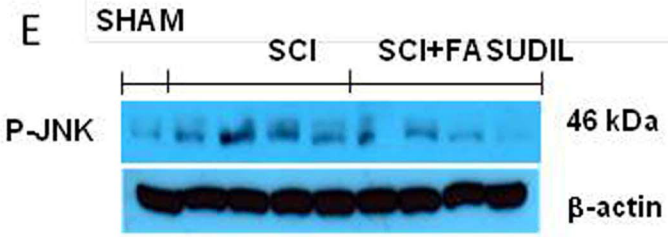

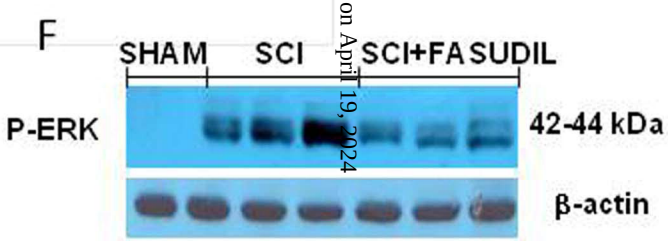

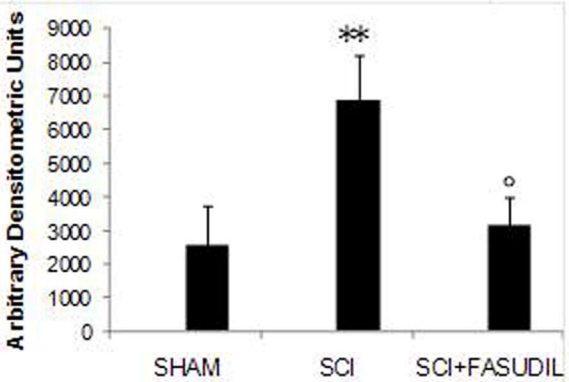

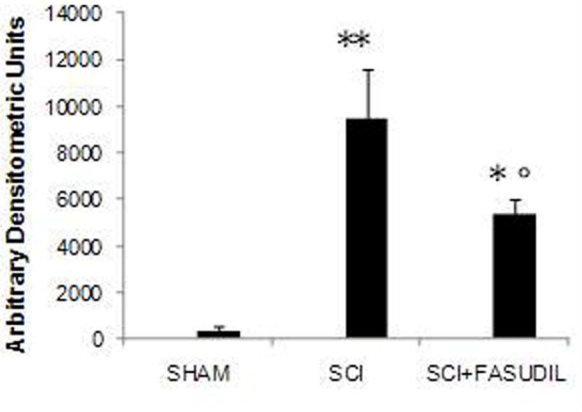

Figure 6

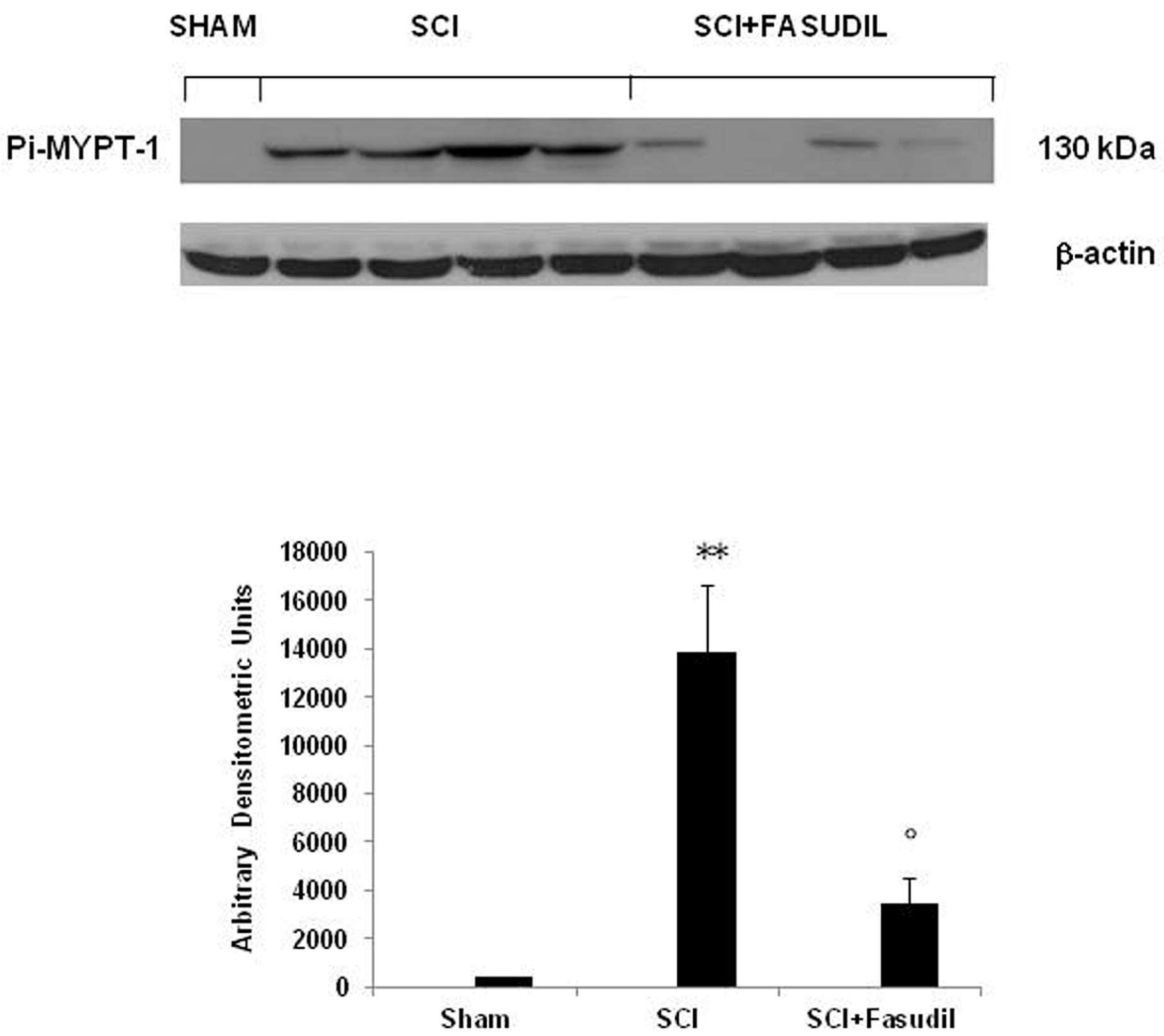

Figure 7

Figure 8

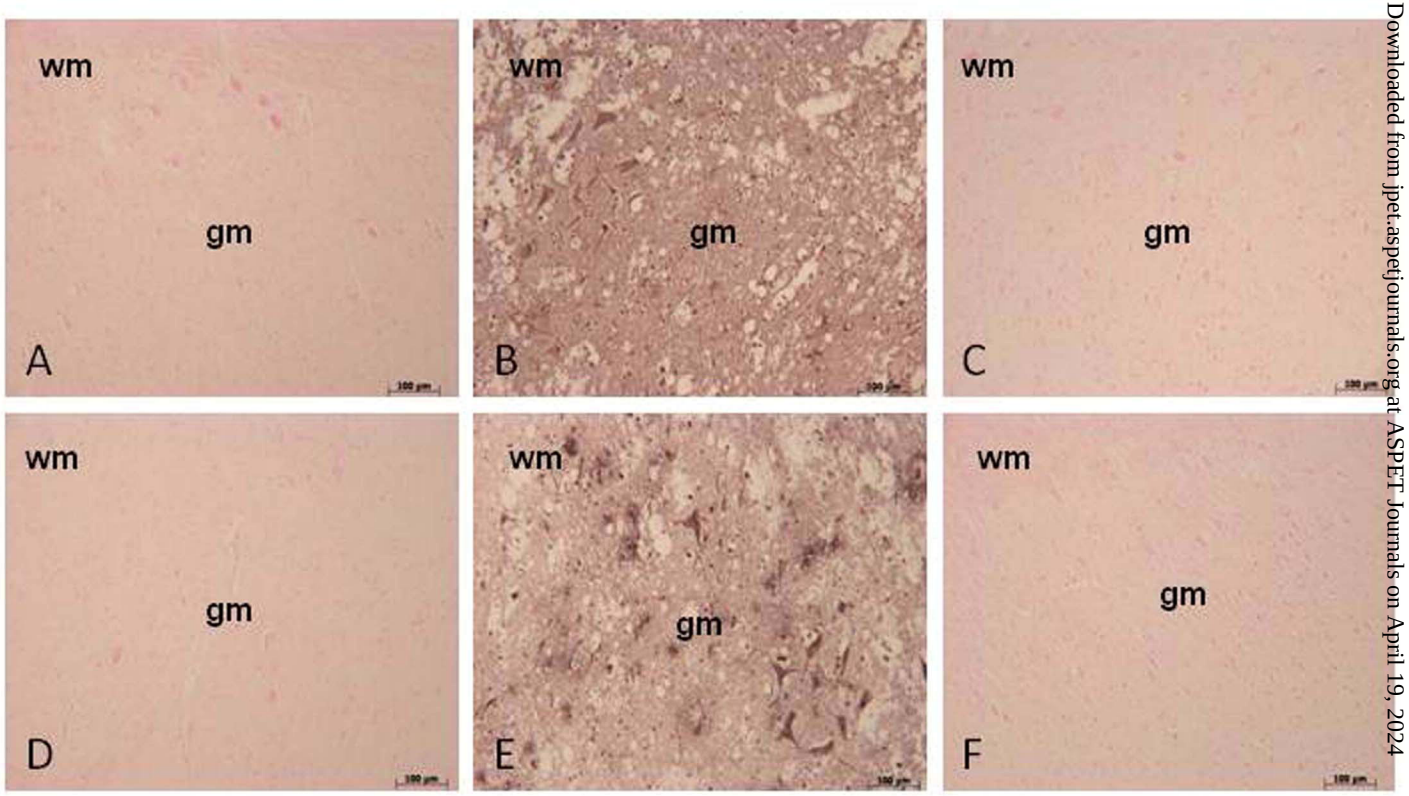

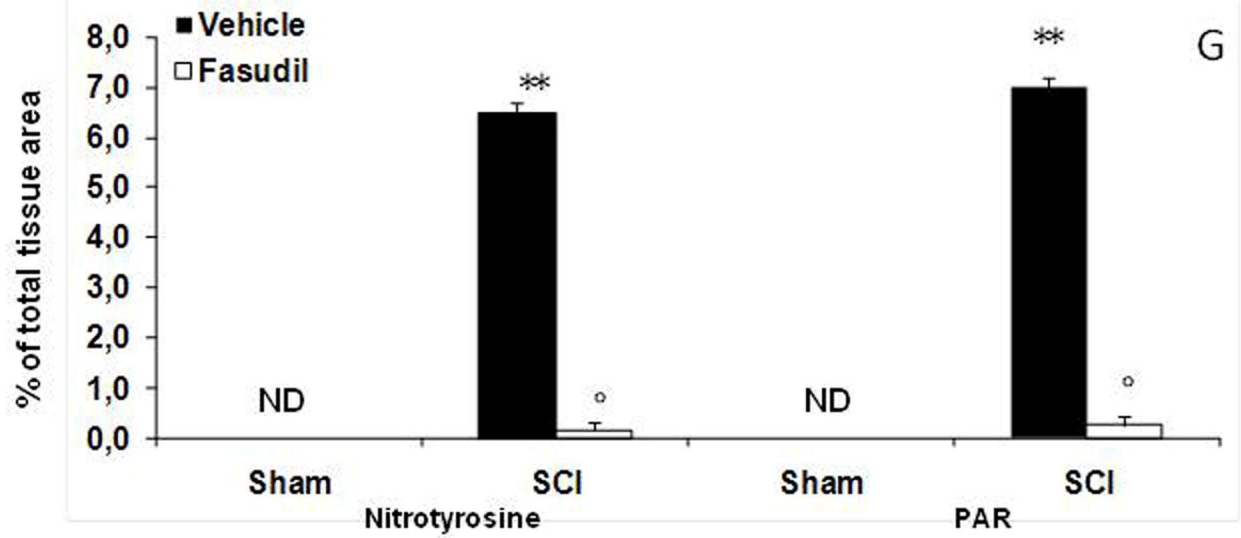

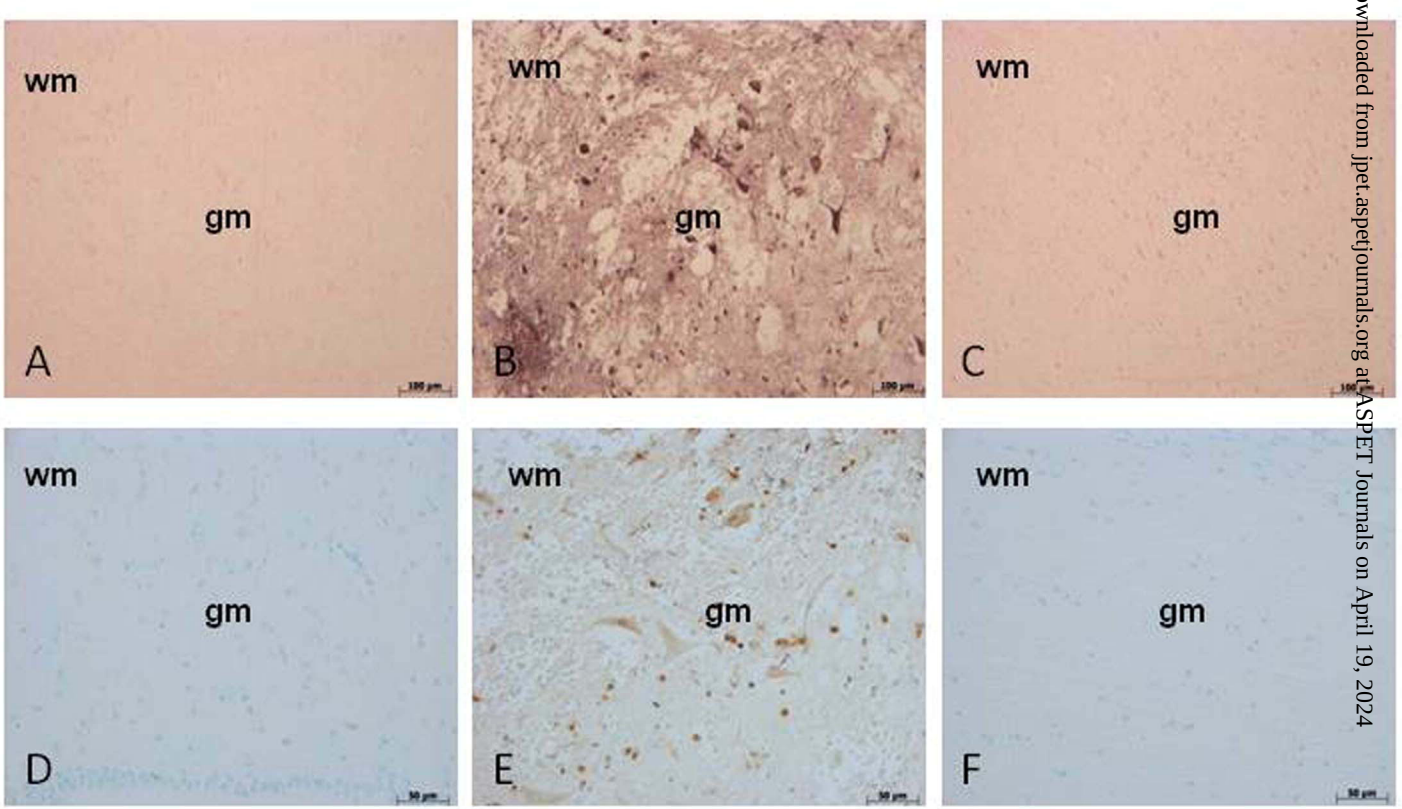

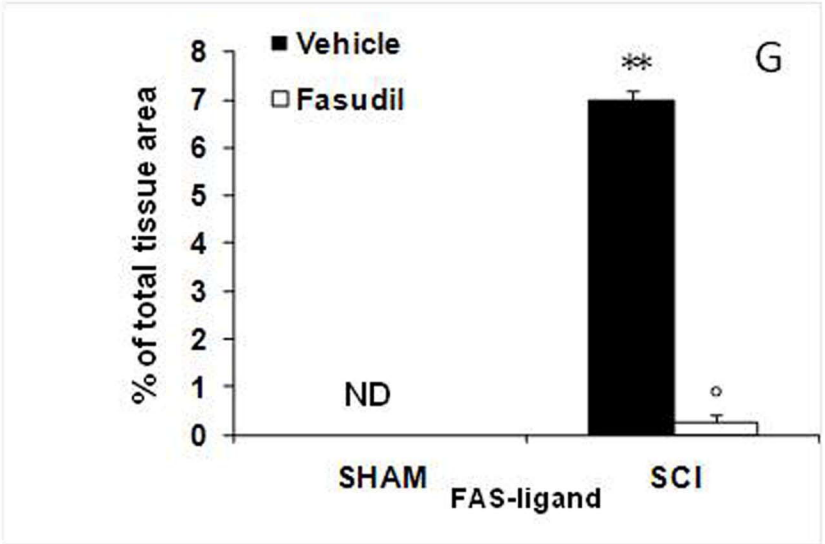

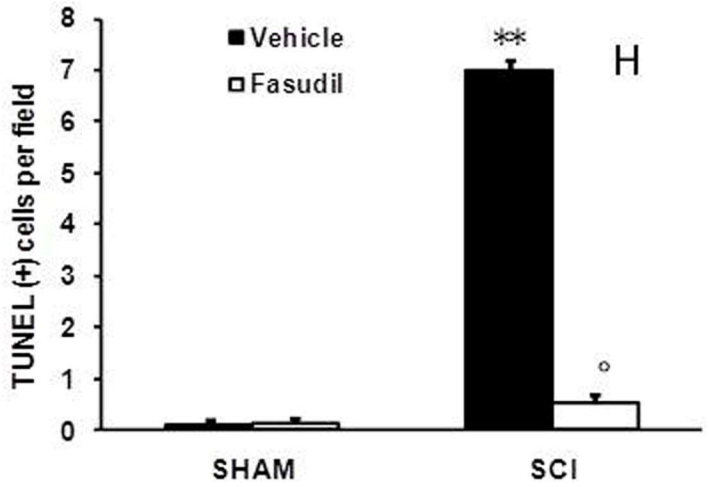

Figure 9

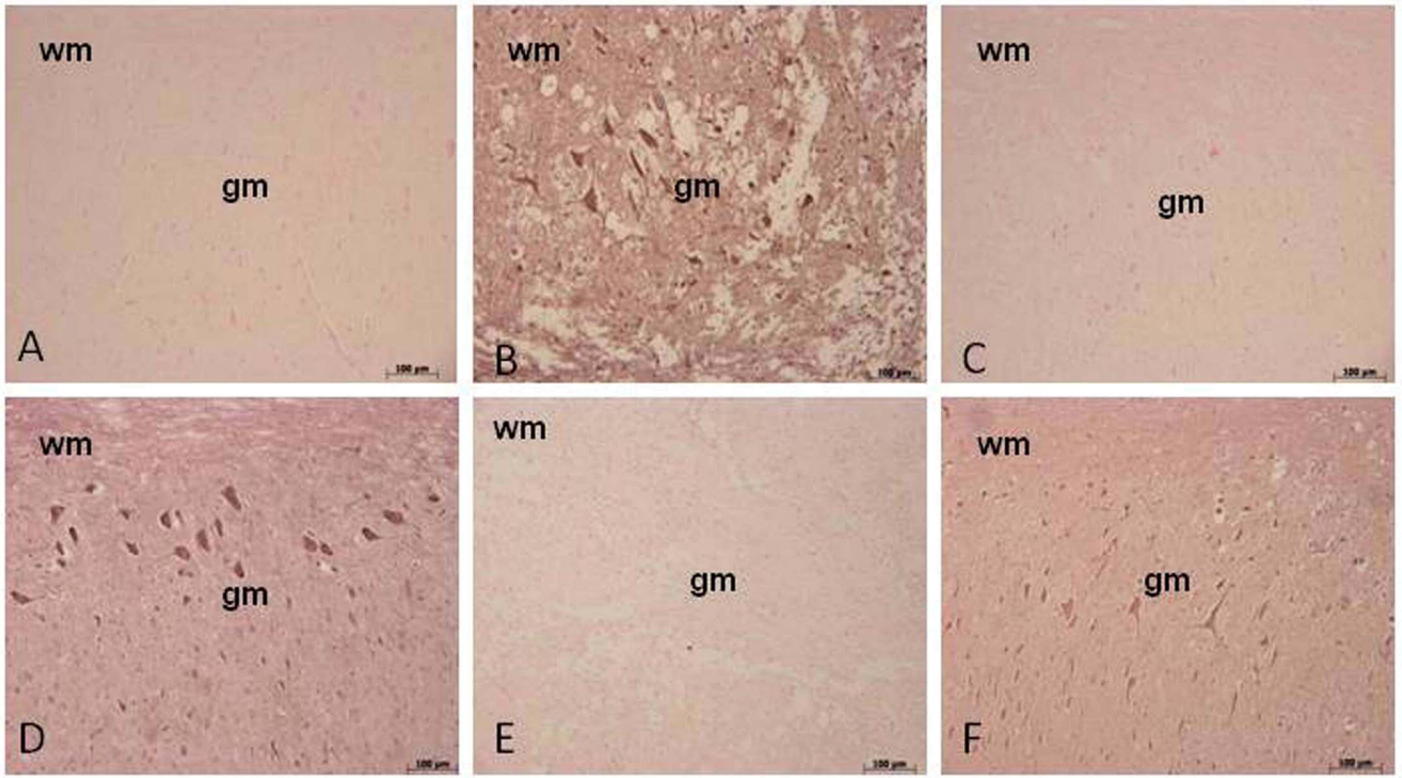

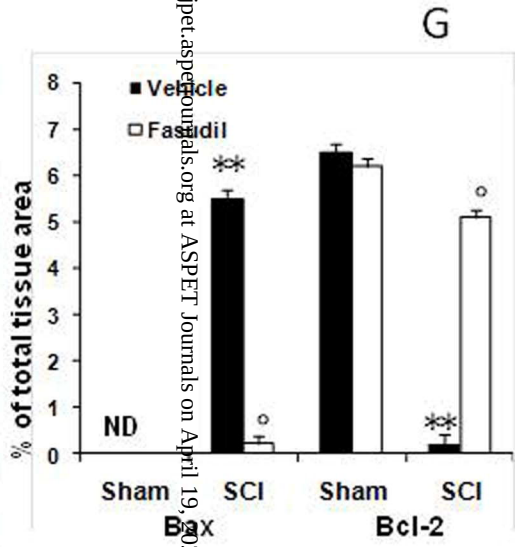

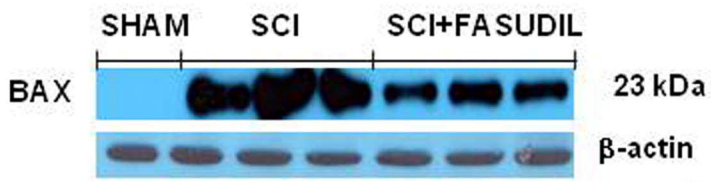

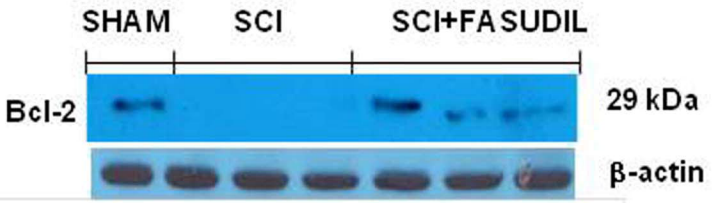

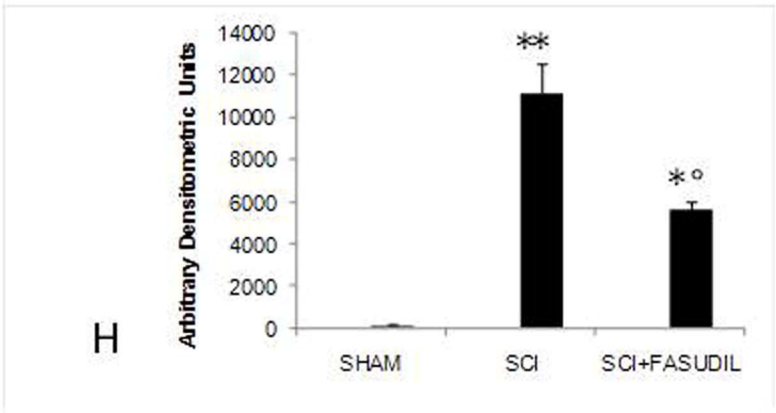

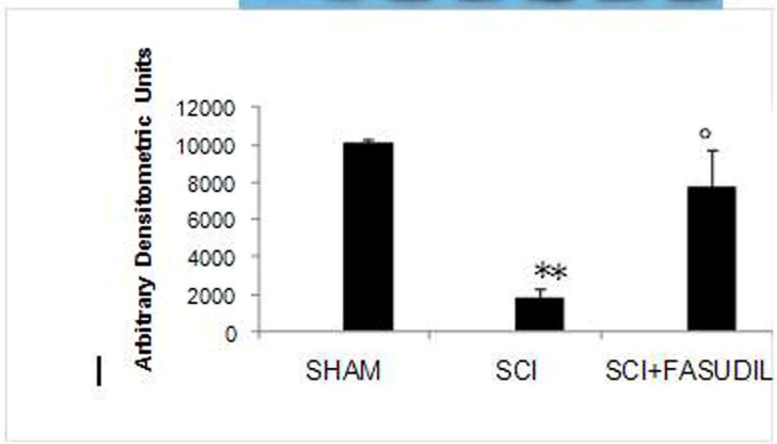

Figure 10